

M. Vorländer

---

## 2.1 Introduction

Acoustic measurements are the obvious prerequisite of acoustic investigations, in research as well as in applied acoustics. They are an important tool for the analysis of acoustical problems or for creation of experimental references in theoretical and numerical approaches. The accuracy required can only be reached if certain requirements concerning the instrumentation are met and if the acoustical conditions and the measurement methods are clearly specified. In applied acoustics, acoustic measurements are often difficult to perform and to interpret. Accordingly, one cannot expect that measured results are absolutely reproducible. Typically, the deviations in repeated measurements are of an order of 1 dB, a magnitude that is acceptable in most cases. These uncertainties are caused by changes in the sound field itself or in the measurement instrumentation.

A measurement arrangement can typically be separated into source and receiver components. The receiver component consists of a ‘sound level meter’ or ‘sound analyser,’ which displays the total sound level in decibels or any other frequency-dependent data. It can also produce results such as ‘spectra’ or ‘impulse responses’. Furthermore, measurements are based on special measurement environments, which allow several reference sound fields to be created.

In this chapter, the components of acoustic measurement instrumentation are explained, together with

the most important measurement quantities and the various techniques of signal processing. Finally, some examples of applications are given.

---

## 2.2 Microphones and Loudspeakers

Almost every acoustic measurement arrangement contains microphones that normally convert sound pressures into electrical signals, which in turn can be displayed, stored, and analysed by analogue or digital techniques. Hence, in a wider sense, other electroacoustical or electromechanical transducers can be called microphones, as well, whereas transducers for underwater sound are called hydrophones, and sensors for structural vibrations, accelerometers.

Microphones for airborne sound contain a very thin and flexible diaphragm, which follows the air movement of the local sound field. The vibration of the diaphragm is converted by the electromechanical force interaction into an electrical signal. In the optimal case, this process is linear and frequency independent.

The electroacoustic conversion yields electrical signals that are proportional to one of the specific sound field quantities, i.e., to sound pressure or to sound velocity. This proportionality depends on whether the sound pressure excites only one or both sides of the diaphragm. In the first case, the electromechanical force on the diaphragm is proportional to the sound pressure, while in the second case it is proportional to the sound pressure gradient.

The sensitivity of a pressure microphone is represented by the open-circuit voltage with reference to the sound pressure on the diaphragm. Each microphone placed into the sound field, however, distorts

---

M. Vorländer (✉)  
Institute of Technical Acoustics, RWTH Aachen University,  
Templergraben 55, 52056 Aachen, Germany  
e-mail: [mvo@akustik.rwth-aachen.de](mailto:mvo@akustik.rwth-aachen.de)

the sound field the more, the larger it is in comparison to the wavelengths of sound. Accordingly, we distinguish between pressure sensitivity and free-field or diffuse-field sensitivity. The latter two are related to the sound pressure in the sound field, without the microphone in place. The frequency responses of pressure and diffuse-field sensitivities differ only slightly, while at high frequencies ( $>10$  kHz) free-field responses are significantly higher by several decibels due to directivity effects.

### 2.2.1 Condenser Measurement Microphones

Condenser microphones are based on the principle of electrostatic transducers, as will be explained in the following. A condenser microphone is a passive electrostatic transducer, consisting of a mobile diaphragm and a rigid backplate. The relation between the mechanical force and the voltage on the condenser is, at first, non-linear, since two charged plates interact with a quadratic law of force and voltage. This is the reason for applying a constant polarisation voltage  $U_0$  (typically 200 V) over a very large resistance  $R$  ( $>10$  G $\Omega$ ). This voltage creates a constant charge on the condenser. A sound-induced modulation of the distance between diaphragm and backplate results in a change in capacity with constant charge, and thus in a sound-induced AC voltage signal  $U$  added to the constant polarisation voltage. For amplitudes that are not too high, the relation between sound pressure and voltage is linear to an excellent approximation. With the measurement microphones used today, this approximation is valid for very high sound pressure levels of up to 140 dB (Figs. 2.1 and 2.2).

The diaphragm typically consists of pure nickel foil of just a few micrometres thick. The dimensions of a

standard measurement microphone are: diameter of 1/2-in. (12.7 mm) and distance between diaphragm and backplate about 20  $\mu\text{m}$ . The capacity of this construction is about 20–30 pF. Furthermore, diameters of 1-, 1/4-, or 1/8-in. are in use. Other dimensions, of course, can be found in studio or miniature recording microphones. For all constructions, the microphone is, in a narrow sense, just the capsule containing the diaphragm, the backplate and the volume. Since the impedance of the capsule itself is extremely high (10–100 G $\Omega$ ), a preamplifier for impedance transformation must be placed near the capsule, so that long cables may be used. Accordingly, the whole arrangement of capsule and preamplifier is called ‘microphone’.

By using a simple equivalent circuit, the sensitivity of a condenser microphone can be estimated in a first approximation. The significant components on the electrical side are resistance and capacity and, on the mechanical side, the compliance of both the diaphragm connected to the housing and of the air cavity. One important task of microphone design is the optimisation of (a) the compliance and (b) the damping of the mechanical resonance caused by holes in the backplate. The resulting frequency response covers a range from 2 Hz to 22 kHz (1/2-in. microphones), and the sensitivity is constant over this range at approximately

$$\frac{U_{I=0}}{p} = nS \frac{U_0}{d}, \quad (2.1)$$

with the open-circuit receiving voltage  $U_{I=0}$  and excitation with the sound pressure  $p$ . The variable  $n$  is the total compliance (diaphragm stiffness and air cavity),  $U_0$  the polarisation voltage,  $S$  the diaphragm surface, and  $d$  the distance from the diaphragm to the backplate. The operation range is limited at low frequencies by electrical and mechanical high pass effects, also by capillary tubes for quasi-static pressure equalisation. At high frequencies, the range is limited by the mechanical resonance of diaphragm mass and total stiffness. The sensitivity of measurement microphones is typically between 10 and 50 mV/Pa, often expressed in terms of  $-40$  dB to  $-26$  dB re 1 V/Pa.

The simplest general type of microphone, usually called a point microphone, has a frequency- and directionally independent sensitivity. In these applications, measurement microphones can be used for all frequencies for which the microphone dimensions are small compared with wavelengths.

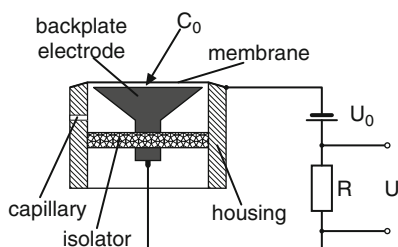


**Fig. 2.1** Principle and equivalent circuit of condenser microphones

For 1/2-in. microphones, this simple approach is valid up to approximately 2 kHz. Above this limit, diffraction at the microphone distorts the sound pressure. The total displacement of the diaphragm is then given by the integral over the surface elements excited by the incident sound wave with locally varying sound pressures in amplitude and phase. Accordingly, the sensitivity is dependent on the direction and describable by a directivity function. This behaviour of microphones must be considered at higher frequencies, and the type of sound field must then be specified.

The polarisation  $U_0$  voltage can be ignored if a dielectric material with permanent polarisation (a so called ‘electret material’) is placed between the condenser electrodes. With electret foils, miniature microphones with dimensions of a few millimetres are available (Table 2.1).

## 2.2.2 Sound Velocity Measurement

For applied acoustics, sound pressure is the most important quantity. For physically correct and complete investigations of sound fields, however, the additional measurement of sound velocities is mandatory, especially for determining field impedances, for solving coupled vibration–radiation problems and, foremost, for measuring sound intensity (see Sect. 2.2.5).

For measuring sound velocity, gradient microphones or, alternatively, combinations of several pressure microphones can be used, e.g., for determining the pressure gradient vector. Using direct velocity sensors is also possible (Fig. 2.3).

Direct velocity sensors based on hot-wire anemometers [1] have proved suitable in practice. This type of sensor is made of platinum resistors, very thin wires that transfer their thermal energy at the operating temperature to the surrounding air when driven at a temperature of 200–400 °C. If a local air flow (sound velocity) is present, the temperature distribution changes asymmetrically, and two closely

mounted wires can be used to detect a local temperature difference and a corresponding voltage difference. The measurement range can be from 100 nm/s to 0.1 m/s.

## 2.2.3 Vibration Sensors

Vibration sensors are receivers for the measurement of structural vibrations. They should be rigidly connected with the surface under investigation. In principle, they consist of a mechanical resonator of a mass  $m$ , a compliance  $n$ , and unavoidable mechanical losses  $w$  (Fig. 2.4).

Let  $x$  be the vibration amplitude of the measurement object and  $x'$  the vibration amplitude of the mass  $m$ . Then the law of momentum conservation gives

$$m \frac{d^2 x'}{dt^2} + w \frac{d}{dt} (x' - x) + \frac{x' - x}{n} = 0, \quad (2.2)$$

or with the differential amplitude  $\xi = x - x'$  and harmonic vibrations:

$$\left( -m\omega^2 + j\omega w + \frac{1}{n} \right) \xi = -m\omega^2 x. \quad (2.3)$$

This equation describes a basic mechanical resonator of mass, spring and damping with the resonance frequency  $\omega_0$ . If highly tuned vibration sensors are used, with

$$\omega_0 = \frac{1}{\sqrt{mn}} \gg \omega, \quad (2.4)$$

the resonator impedance is dominated by the compliance. This simply yields

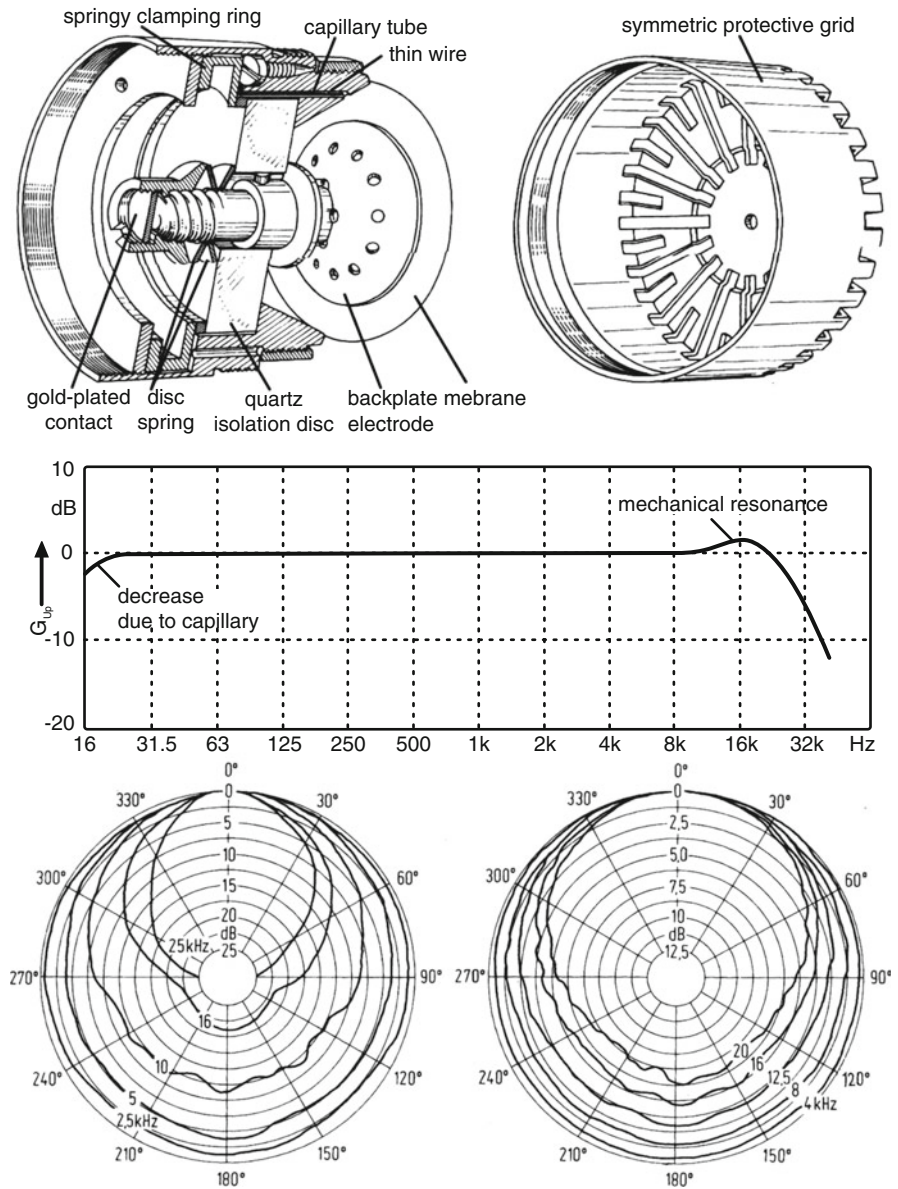
$$\xi = -mn\omega^2 x = -\left( \frac{\omega}{\omega_0} \right)^2 x, \quad (2.5)$$

from which follows that the quantity to be observed,  $\xi$ , is proportional to the acceleration of the measurement surface,  $\omega^2 x$  (Fig. 2.5).

**Table 2.1** Technical data for several microphones

Type	Durchmesser mm	Übertragungsfaktor $10^{-3}$ V/Pa	Frequenzbereich Hz	Dynamikbereich dB(A) re $2 \cdot 10^{-2}$ Pa
Kondensator 1/8□	3,2	1	6,5...140k	55...168
Kondensator 1/4□	6,4	4	4...100k	36...164
Kondensator 1/2□	12,7	12,5	4...100k	36...164
Kondensator 1□	23,8	50	2,6...18k	11...146
Dauerpol. 1/2□	12,7	50	4...16k	15...146
Elektrodyn.	33	2	20...20k	10...150

**Fig. 2.2** Condenser microphone. (a) Construction sketch; (b) Frequency response; (c) directional characteristics



It is essential that the mass impedance  $\omega m$  of the acceleration sensor is small compared with the impedance of the measurement object. Therefore, when measuring on small impedances, for instance, those of light and soft construction elements, the limits related to the mass and mounting of the sensor must be taken into account. The maximum permissible sensor mass  $M$  can be estimated by

$$M < 0.36 \sqrt{10^{\Delta L/10} - 1} \rho c_L h^2 / f, \quad (2.6)$$

with  $c_L$ ,  $\rho$ , and  $h$  being longitudinal wave speed, density, and thickness of the measurement object

(plate), respectively, and  $\Delta L$  being the maximum permissible error. Depending on the way the sensor is mounted, the connection of sensor and surface can be interpreted as an additional spring. If measurements are to be performed at high frequencies, a very stiff connection is necessary, possibly by using screws. If only low frequencies are of interest, connections with wax or contact pins are sufficient.

In building acoustics, the range of surface displacements and the corresponding accelerations can be extremely large, covering vibrations of thin sheet metal or of massive walls. The sensitivities, masses, mounting and the relevant frequency ranges

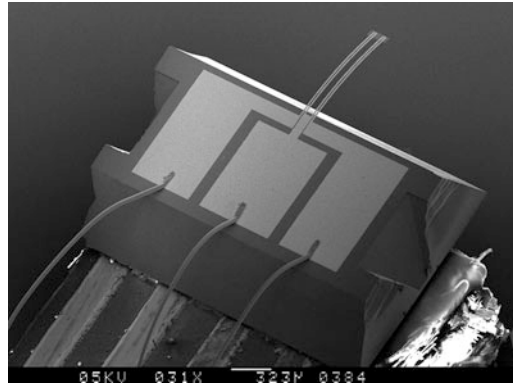


**Fig. 2.3** Scanning electron microscope image of a velocity sensor (Microflow [1]) according to the hot-wire anemometer. The diameter of the wire (aluminium) is  $80\ \mu\text{m}$

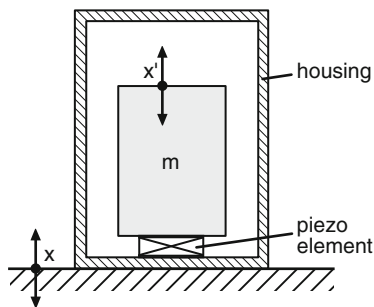


**Fig. 2.4** Construction sketch of an accelerometer

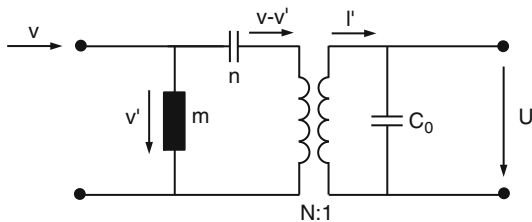


**Fig. 2.5** Equivalent circuit of an accelerometer

must be specifically chosen in each case. This is, however, not problematic due to the large variety of commercially available accelerometers.

One very elegant but also quite sophisticated instrumentation is based on optical measurement methods, for instance by using laser-Doppler vibrometers. They are typically based on the principle of a Mach-Zehnder interferometer, which not only makes use of optical interferences caused by phase differences but also of the Doppler frequency shift. Hence, extremely small displacements can be

measured accurately. If the laser beam is reflected or scattered by the measurement object, the reflected wave is shifted in phase and frequency. The problem then is to measure the rather small laser light frequency shift by beating a reference beam with the reflected beam and by measuring the intensities with a photo detector. It is thus possible to resolve vibration amplitudes, which are smaller than the light wavelength. This method was successfully applied, for instance, for measurement of microphone diaphragms or eardrums, although the displacement amplitudes are of orders of magnitude of just nanometers.

## 2.2.4 Microphone Calibration

In applied acoustics, the most frequently used method for calibration of the instrumentation makes use of so called ‘pistonphones’ or sound calibrators (see Sect. 2.2.4.1 below). Almost everyone who uses a measurement microphone will test its function with a sound calibrator. To achieve this goal, the user must be absolutely sure that the calibrator is working well. The manufacturer of the instrumentation, together with calibration authorities and reference laboratories, are responsible for assuring quality. This chain of measurement and calibration is called ‘traceability’ of measurement standards, finally connected to a primary standard, including an absolute primary calibration.

The calibration of an electroacoustic transducer can be performed in four different ways, by using: (1) a calculated mechanical or optical effect in the sound field, (2) a theoretically ‘known’ sound field (see

Sect. 2.2.4.1), (3) a reference microphone (see Sect. 2.2.4.2), and (4) the reciprocity principle (see Sect. 2.2.4.3).

Furthermore, there is a simple procedure for relative calibration and for quality control in production, namely the electrostatic actuator technique. An electrostatic actuator is a plate with an adapter ring, which is mounted directly on the microphone (instead of the protection grid). With an AC voltage on the actuator, the diaphragm is excited by a quasi-electrostatic force. The received voltage at the output terminals of the microphone is approximately proportional to the voltage, which would occur in the pressure sound field in an acoustic coupler. Accordingly, the sensitivity determined with the actuator gives an approximate figure for the pressure sensitivity.

### 2.2.4.1 Sound Calibrators

A vibrating piston in a pressure cavity (coupler) produces a sound field of known sound pressure (Fig. 2.6). The sound calibrator and the pistonphone are based on this principle. With a displacement amplitude  $\hat{\xi}$ , the pressure amplitude in the cavity volume is

$$\hat{p} = \frac{\rho_0 c^2}{V_0} S \hat{\xi}. \quad (2.7)$$

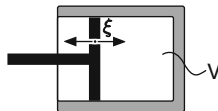
We assume that all dimensions are small compared to the wavelength and that the boundaries of the cavity are rigid.  $V_0$  is the cavity volume and  $S$  is the piston area. Then the microphone sensitivity is the ratio of the output voltage and the sound pressure amplitudes:

$$M = \frac{\hat{U}}{\hat{p}} = \frac{V_0}{\rho_0 c^2 S} \cdot \frac{\hat{U}}{\hat{\xi}}. \quad (2.8)$$

### 2.2.4.2 Comparison Methods

Comparison methods are usually very easily applied. We excite a reference microphone and the microphone under test one after the other, and we get the difference between the two sensitivities directly. Knowing the absolute sensitivity of the reference microphone,

**Fig. 2.6** Principle of the pistonphone



gives us the sensitivity of the tested microphone. Consequently, the reference microphone or ‘standard microphone’ must be available. This must have previously been absolutely calibrated with a precision method or, at least, compared with a primary standard. Comparison methods are usually applied by calibration services or similar authorities that are responsible for sound level meter and microphone testing. These measurements are related to (coupler) pressure fields, for instance, for microphones in headphone couplers (artificial ears) for audiometer calibration. In the case of free field or diffuse field calibrations, the devices tested are typically sound level meters for noise immission control and for building acoustics.

The standard measurement microphones are compared with national or internationally agreed upon standards of legal metrology or are calibrated with primary methods. Any microphone of the latter kind must be calibrated with a primary method such as the reciprocity method (Fig. 2.7).

### 2.2.4.3 Reciprocity Calibration

The most exact, variable, and reliable calibration method is the reciprocity method. It is performed in several steps. The reciprocity principle is one of the basic principles of reversible transducers, best explained by electroacoustic four-poles. The electrostatic and the electrodynamic transducer follow that principle:

$$\left(\frac{p}{I}\right)_{Q=0} = \left(\frac{U}{Q}\right)_{I=0} \quad (2.9)$$

$$\left(\frac{U}{p}\right)_{I=0} = -\left(\frac{Q}{I}\right)_{p=0},$$

where  $Q$  = volume velocity or, volume flow in  $\text{m}^3/\text{s}$ . Of specific importance is the second equation, which

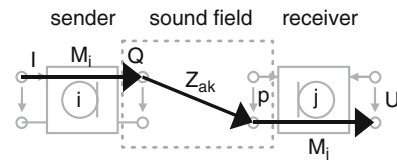


**Fig. 2.7** Equivalent circuit with electrical and acoustical two-ports representing an arrangement of two microphones in reciprocity calibration and definition of transfer impedance:  $Z_{ij} = M_i \cdot Z_{ak} \cdot M_j$

relates the sensitivity factor of the transduction between the source,  $Q/I$ , and the receiver,  $U/p$ . Both quantities are generally frequency dependent and complex, for instance  $U = \underline{U}(f)$ :

$$M = \frac{U_{I=0}}{p} = -\frac{Q_{p=0}}{I}. \quad (2.10)$$

It shall be noted, however, that the sensitivity in the receiving case (sensitivity factor  $M$ ) is not defined in exactly the same way as the so-called ‘sensitivity’ sources such as of loudspeakers. The latter is not related to the volume velocity of the microphone diaphragm but to the sound pressure in the far field. Accordingly, it contains the radiation function (Green’s function).

A further basic quantity of reciprocity calibration is the electrical transfer impedance  $Z_{ij}$  of a transfer four-pole consisting of two microphones ( $i$  and  $j$ ) coupled over an acoustic path. Microphone  $i$  is driven as source and microphone  $j$  as receiver.  $U_j$  is the open-circuit receiving voltage and  $I_i$  the source current. By definition, this is

$$Z_{ij} = \frac{U_j}{I_i}. \quad (2.11)$$

The electrical transfer impedance can also be formulated by means of the two sensitivity factors  $M_i$  and  $M_j$ , which are independent of the direction, and by the acoustic transfer impedance  $Z_{ac}$ . This then yields

$$Z_{ij} = \frac{U_j}{I_i} = M_i \cdot Z_{ac} \cdot M_j. \quad (2.12)$$

With this equation and measurement of the electrical transfer impedance, the product of two sensitivity factors can be determined if the acoustic transfer impedance (Green’s function) is known. Equation (2.12) contains two unknowns ( $M_i$  and  $M_j$ ). Two measurements with exchanged source and receiver are redundant due to reciprocity  $Z_{ij} = Z_{ji}$ , but three measurements on three microphones  $i, j$  and  $k$  in pairs give the result of the three microphone sensitivity factors  $M_i, M_j$  and  $M_k$  by calculating

$$M_i = \sqrt{\frac{1}{Z_{ak}} \frac{Z_{ij}Z_{ik}}{Z_{jk}}}, \quad (2.13)$$

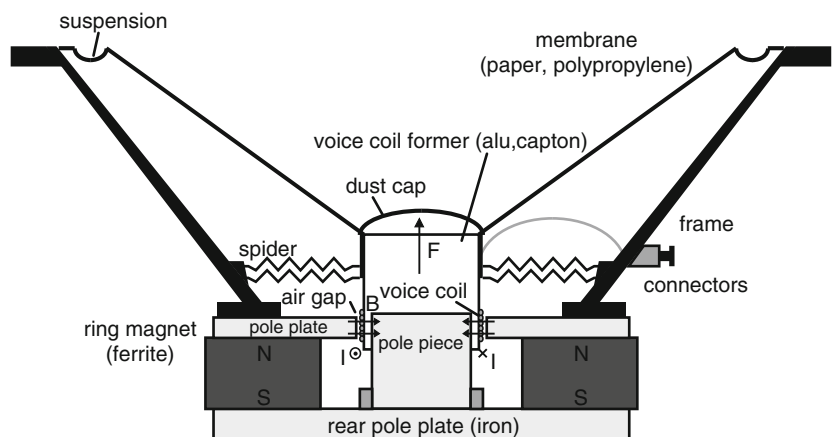
as well as two more equations of the same kind with a cyclic exchange of  $i, j$ , and  $k$ .

Under free field and diffuse field conditions, the acoustic transfer impedance can be easily calculated. The practical conditions, however, of the signal-to-noise ratio are extremely difficult, due to very low acoustic signal levels. However, the most accurate acoustic measurement is the pressure reciprocity calibration in small acoustic cavities. The cavity is considered small compared with the wavelength. In this simple consideration, the closed cavity with volume  $V_0$  behaves mechanically like a spring:

$$Z_{ac|cavity} = \frac{\kappa p_0}{j\omega V_0}. \quad (2.14)$$

For precision calibrations, several thermodynamic corrections (atmospheric pressure, heat conduction, etc.) must be added. Furthermore, extensions of Eq. (2.14) concerning the equivalent volumes of the

**Fig. 2.8** Electrodynamic loudspeaker



microphone diaphragms, higher-order modes and waveguide models in cylindrical couplers must be used.

## 2.2.5 Intensity Probes

Sound intensity is an important quantity for evaluating and localising sound sources and sound absorbers and for determining physical sound field properties. It can give information about the type of waves and about the acoustic energy flow. Furthermore, it can be used for measuring the sound power of sources, provided the intensity is obtained over a closed surface surrounding the source.

Intensity probes must deliver the sound pressure  $p$  and the sound velocity  $v$  simultaneously. This is achieved by using a p–u probe, in which a condenser microphone is closely coupled to a velocity sensor according to the ultrasound Doppler principle [2] or to an anemometer (see Sect. 2.2.2). Much more common is the so-called p–p probe consisting of two condenser microphones placed either face to face or side by side. The sound pressure measured by this probe is

$$p(t) = \frac{p_1(t) + p_2(t)}{2}. \quad (2.15)$$

For determining the sound velocity, the basic force equation

$$\text{grad}p + \rho \frac{\partial v}{\partial t} = 0, \quad (2.16)$$

is approximated by the finite differences (in the  $x$  direction)

$$\frac{\Delta p}{\Delta x} + \rho \frac{\Delta v}{\Delta t} = 0, \quad (2.17)$$

and thus the component of the sound velocity in direction  $x$  can be expressed as

$$v(t) = -\frac{1}{\rho} \int_{-\infty}^t \frac{p_2(\tau) - p_1(\tau)}{\Delta x} d\tau. \quad (2.18)$$

The component of the active sound intensity in the direction of the pressure gradient is thus:

$$I_r = \overline{p(t)v(t)} = \frac{1}{2\rho\Delta x} \frac{1}{T} \int_0^T [p_1(t) + p_2(t)] \int_0^t [p_1(\tau) - p_2(\tau)] d\tau dt, \quad (2.19)$$

with  $T =$  averaging time (see Sect. 2.3.1). By Fourier transformation, the same circumstances can be expressed in the frequency domain by Fourier transformation in terms of the imaginary part ( $\Im$ ) of the cross power spectrum  $G_{12}$ :

$$I_r = -\frac{1}{\omega\rho\Delta x} \Im\{G_{12}(f)\}. \quad (2.20)$$

Determining the sound velocity with velocity sensors or with microphone pairs yields only one component of the sound intensity, which is the nominal direction of the probe. If the direction of sound intensity shall be determined also, spatial probes must be applied, for instance as an arrangement of several microphone pairs, oriented orthogonally or multi-microphone probes on regular polyhedra [3].

However, here it must be considered that more complex probes produce larger errors concerning the acoustic centre and the spatial resolution, since pressure and velocity are not strictly measured at the same point. The construction and calibration of sound intensity probes must be performed very carefully, because the differences in sensitivities and, particularly, in relative phases of the transducers produce apparent pressure gradients or contributions to  $G_{12}$  and influence the measurement result.

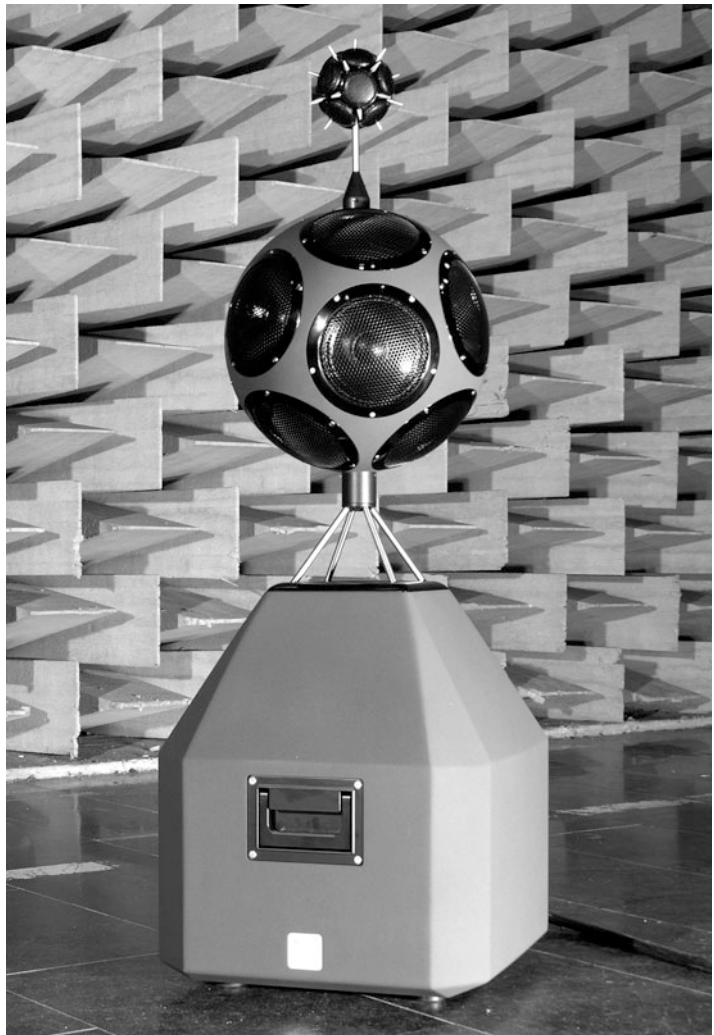
For example, a fully reactive sound field can be used for evaluating the quality of sound intensity probes. The energy flow and the active sound intensity must be zero. This applies, for example, to standing waves. The relative phase between pressure and velocity is  $\pi/2$ , and the instantaneous intensity  $p(t) \cdot v(t)$  is proportional to  $\sin(\omega t) \cdot \cos(\omega t) \propto \sin(2\omega t)$ , which is zero in temporal average. This example illustrates that the phase between pressure and velocity must be

measured very accurately. The relative phase results in the end from the phase difference between the pressure microphones or between the pressure and the velocity sensor. Therefore, high standards must be set for the transducers and the connected circuits, such as analogue input sections and filters of the analysers. Phase errors are significant in p-p probes, if the pressure gradient is small, i.e., if the microphone distance is too small compared to the wavelength. For quality control of intensity probes and analysers [typically real-time analysers are applied to calculate Eqs. (2.19) or (2.20)], special calibrators and a set of field indicators [4] are available, which give information, for instance, about the smallest measurable sound intensity (residual intensity).

### 2.2.6 Loudspeakers

The classical measurement loudspeaker principle is based on the dynamic transducer. An electrodynamic loudspeaker consists of a conical membrane, which in its centre is connected to a cylindrical voice coil. The coil is placed in the air gap of a pot magnet of hard magnetic ferrite or of Alnico alloy, in which a radially homogeneous magnetic field is established by a magnetic flux density of some  $Vs/m^2$ . The resistance of the coil is typically several Ohms; at higher frequencies the inductance is significant, too. The latter can be reduced by copper rings in the air gap, which at the same time add damping to the mechanical resonance (Fig. 2.8).

**Fig. 2.9** Dodecahedron loudspeaker



The movable parts of the loudspeaker (the membrane and voice coil) are supported by springs. This is realised by a spider to keep the voice coil in the nominal position and by a soft mounting of the membrane at its outer perimeter. The membrane is made of a material with high internal damping and low density in order to suppress bending waves. The common material is paper, but today PVC or light metals are also used.

Due to the relatively large mass of the vibrating parts and due to the mechanical system's resonance, the impulse onset of dynamic loudspeakers is typically not acceptable. This limits the possibility of generating short pulses. It can be improved by adequate damping (low impedance of the connected power amplifier). However, with modern methods of digital signal processing and inverse filtering, the system parameters can be optimised and an absolutely linear sound reproduction in a wide frequency range can be obtained. Particularly because loudspeaker equalisation can be realised rather well, loudspeaker optimisation is to be focussed on improvement of the directivity of radiation.

Nonlinear distortions of dynamic loudspeakers result from the nonlinear stiffness of the membrane support, from inhomogeneities of the magnetic field and from the Doppler shift, if signals contain low and high frequencies simultaneously (broadband signals). Since they are relatively small, the dynamic loudspeaker is the most frequently used loudspeaker type.

Improvement of radiation at low frequencies is gained by using loudspeaker boxes; however, with the side effect that the system resonance shifts to higher frequencies. The resonance frequency sets the low frequency limit. Thus it is important to match the loudspeaker system with the box dimensions. The radiation directivity and the axial sound field, estimated from the radiation of a piston mounted in a baffle, can be used as an approximation for the sound field of loudspeaker boxes. Then, however, diffraction at the box edges is an additional factor influencing the far field sound pressure.

### 2.2.6.1 Special Measurement Loudspeakers

In many acoustic measurements, the goal is to produce plane waves or an approximation of particular types of sound fields. Plane waves can be produced by common loudspeakers quite well, if the measurement area is on the main radiation axis of the far field and on a small area. The result will be better (a) if the loudspeaker membrane area  $S$  is small, since the far-field distance

$$r_F \approx \frac{S}{\lambda} = \frac{Sf}{c}, \quad (2.21)$$

in this case is very small and (b) with coaxial multiple loudspeakers, which have a common axis of radiation. Such systems concentrate the radiation on the main axis, but the wavefront in far field is symmetrical and approximately plane and is constant in level (many measurement standards assume plane wave conditions with  $p$  and  $v$  in phase at a distance of 2 m).

Special directivities are necessary for artificial singers or speakers, for instance, in the measurement of headsets, communication devices or Lavalier microphones. For these purposes, loudspeakers that radiate the sound from a mouth opening and an artificial human diffraction body (head and torso simulator, artificial singer) can be used.

If one does not want any specific directivity pattern but an omnidirectional radiation, particular methods of loudspeaker construction must be followed, as well.

Provided that the loudspeaker dimensions are not very small compared to the wavelength, then an omnidirectional radiation can at least be approximated by loudspeakers in spherical symmetry by means of housings based on regular polyhedra (tetrahedron, cube, dodecahedron, icosahedron with 4, 6, 12, or 20 loudspeaker systems, respectively). The dodecahedron is most commonly used (Fig. 2.9).

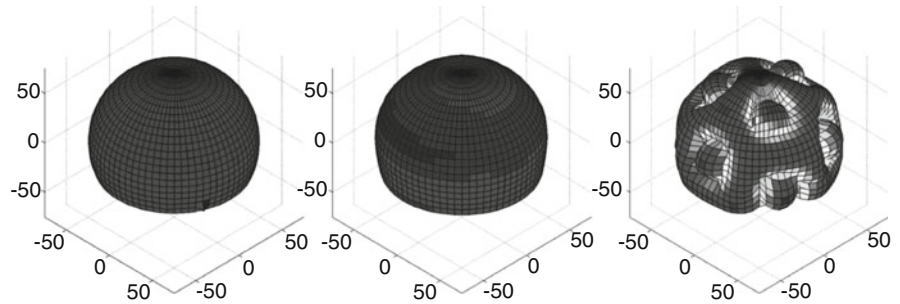
The illustration of the pure-tone directivity patterns of dodecahedrons is difficult to interpret, because broadband signals are more likely required in acoustic applications. It is thus reasonable to use three-dimensional illustrations of the directionally radiated sound pressure in terms of frequency-averaged spectra (Fig. 2.10).

## 2.3 Sound Level Measurement and Rating

Generally, almost every acoustic instrumentation can be divided into a source component and a receiving component. The receiving component is a sound level meter or, more generally, a sound analyser. This component displays either the total sound level in decibels or it performs a frequency analysis and displays a 'spectrum'.

The basic quantity to be considered is the sound pressure level (see Sect. 2.1):

**Fig. 2.10** Directivity of a dodecahedron loudspeaker. One-third octave band analysis at centre frequencies of 100 Hz, 1 kHz and 10 kHz (left to right)



$$L = 20 \log \left( \frac{\tilde{p}}{p_0} \right); p_0 = 2 \times 10^{-5} \text{ N/m}^2, \quad (2.22)$$

where  $\tilde{p}$  is the rms sound pressure determined over an averaging time  $T_m$  according to

$$\tilde{p} = \sqrt{\frac{1}{T_m} \int_0^{T_m} p^2(t) dt}. \quad (2.23)$$

from a sound pressure time function  $p(t)$ . For instance,

$$p(t) = \hat{p} \sin \omega t, \quad \tilde{p} = \frac{\hat{p}}{\sqrt{2}}. \quad (2.24)$$

According to the formula for the effective sound pressure, the term ‘rms’= root [mean (square)] can be easily remembered.

### 2.3.1 Averaging Times

It cannot be generally assumed that the sound signal to be measured is periodic (Fig. 2.11). The averaging time is therefore not unique and must be specified beforehand. The duration of the averaging  $T_m$  is dependent on whether the signal  $p(t)$  is pulse like or stationary. International standards have fixed the application of two main time constants: 125 ms (=‘FAST’) or 1 s (=‘SLOW’). SLOW has the advantage that the sound pressure level is rather stable and is easily readable from the display. Pulsive sound, however, is smoothed significantly. Beside FAST and SLOW, there are other (also unsymmetrical) time averages. Furthermore, it is important to consider a quantity for the evaluation of long-term noise exposition, represented by the energy equivalent sound

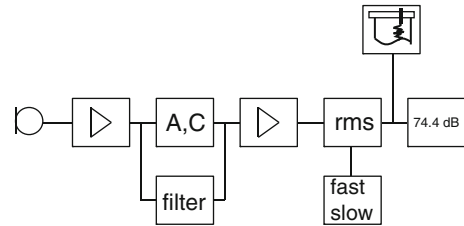


**Fig. 2.11** Components of a sound level meter. Left to right: Microphone, preamplifier, A, C, or bandpass filter, amplifier, rms detector (time constants), display or level recorder

pressure level  $L_{eq}$ . In order to describe the total sound energy exposure, the averaging time can last from several seconds up to several hours. The latter application occurs in noise abatement, in working environments (8 h) and in industrial or urban noise control (day and night periods).

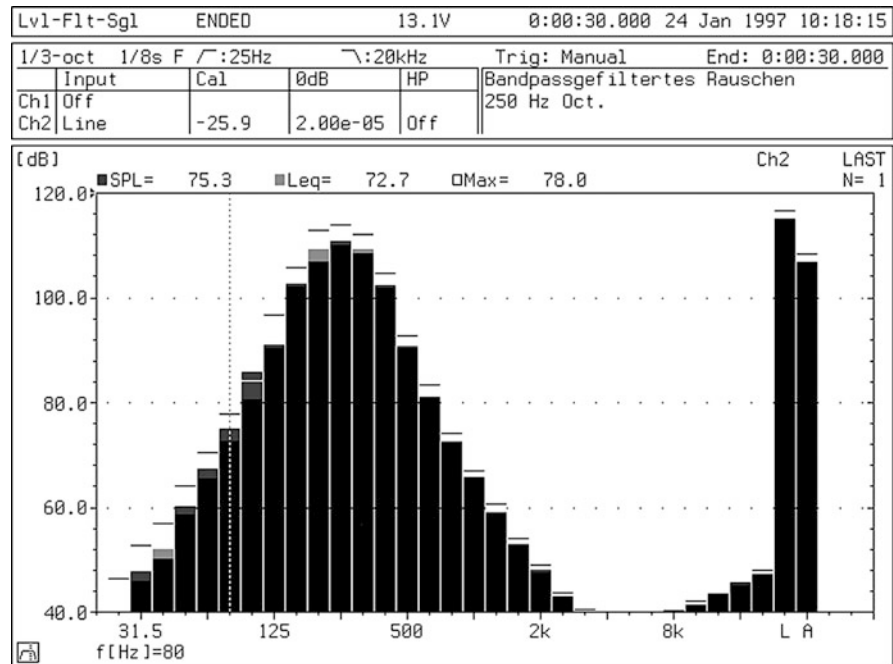
### 2.3.2 Frequency Rating

A second, very important averaging procedure is frequency rating. Here we try to take into account the frequency dependence of human hearing. Historically, the so called ‘A-weighting’ and indication of ‘dB(A)’ became the leading quantity. The meaning of dB(A) is that the sound level meter is extended with a standardised bandpass filter which simulates the frequency curve of the equal loudness contour  $L_N$  at 20 phon (Table 2.2).

The filters are, however, strongly simplified in order to ensure a feasible realisation with elementary circuits. B and C weighting is also specified to simulate equal loudness contours at higher levels.

The choice of time and frequency rating is specified in each individual case of measurement. An exact indication of the type of sound level in terms of indices is advisable, for instance,  $L_{AF}$ ,  $L_{A,eq}$ , or  $L_{CS}$ .

**Fig. 2.12** Display of a real-time frequency analyser



### 2.3.3 Precision

Sound level meters for the measurement of absolute sound levels must fulfil several requirements. Before a qualified sound level meter is purchased, these are checked in type testing or in type approval tests, where acoustic and electric tests are performed (internationally standardised in IEC 60651). The goal of the control system is a correct and reliable result of the sound level, independent of conditions such as temperature or moisture. Another goal is the exact description of the application of the instrument in the sound field (directivity, calibration with pistonphone, etc.). The electrical test includes, in addition to other tests, excitation of the rms detector with several signals to check the correct implementation of the time and frequency ratings. Depending on the quality, the sound level meter is then placed into class 0, 1, 2, or 3 (see Table 2.3).

### 2.3.4 Bandpass Filters

A modern but more complicated method of sound level measurement is frequency analysis in frequency bands, typically in one-third octave bands or in octave bands. A traditional sound level meter can be extended

by a set of bandpass filters to determine the sound pressure level for a specific frequency band. If the sound event is not stationary, however, the bandpass filters must be used at run-time in parallel. This is implemented in a real-time frequency analyser (Fig. 2.12). The midband frequencies of one-third octave bands are defined on a logarithmic frequency scale as follows (here in the example of the base 2 logarithm):

$$\begin{aligned}
 f_u &= 2^{1/3} \cdot f_l \\
 \Delta f &= f_u - f_l = f_l (2^{1/3} - 1) \\
 f_m &= \sqrt{f_l \cdot f_u} \\
 f_{m+1} &= 2^{1/3} f_m,
 \end{aligned} \tag{2.25}$$

with  $f_l$  and  $f_u$  as lower and upper edge frequency and  $f_m$ ,  $f_{m+1}$  as midband frequencies of the bands  $m$  and  $m + 1$ .

Similarly, for octave bands

$$\begin{aligned}
 f_u &= 2f_l \\
 \Delta f &= f_u - f_l = f_l \\
 f_m &= \sqrt{f_l \cdot f_u} = \sqrt{2}f_l \\
 f_{m+1} &= f_m \cdot 2.
 \end{aligned} \tag{2.26}$$

Formerly, one-third octave bands and octave bands were designed using analogue Butterworth filters,

**Table 2.2** Table of standard frequencies and A-weighting

Nominal frequency in Hz	Exact frequency (base 10) in Hz	A-weighting
10	10,00	-70.4
12.5	12.59	-63.4
16	15.85	-56.7
20	19.95	-50.5
25	25.12	-44.7
31.5	31.62	-39.4
40	39.81	-34.6
50	50.12	-30.2
63	63.10	-26.2
80	79.43	-22.5
100	100	-19.1
125	125.9	-16.1
160	158.5	-13.4
200	199.5	-10.9
250	251.2	-8.6
315	316.2	-6.6
400	398.1	-4.8
500	501.2	-3.2
630	631.0	-1.9
800	794.3	-0.8
1,000	1,000	0.0
1,250	1,259	+0.6
1,600	1,585	+1.0
2,000	1,995	+1.2
2,500	2,512	+1.3
3,150	3,162	+1.2
4,000	3,981	+1.0
5,000	5,012	+0.5
6,300	6,310	-0.1
8,000	7,943	-1.1
10,000	10,000	-2.5
12,500	12,590	-4.3
16,000	15,850	-6.6
20,000	19,950	-9.3

**Table 2.3** Precision classification of sound level meters

Class	Application	Uncertainty limit
0	Laboratory, standard reference	$\pm 0.4$ dB
1	Laboratory, field measurement	$\pm 0.7$ dB
2	General field measurement	$\pm 1.0$ dB
3	Survey measurement	$\pm 1.5$ dB

whereas today, digital filters have replaced the analogue solutions. Mostly the filters are constructed as IIR filters (IIR = infinite impulse response), also as digital representatives of Butterworth filters. The

realisation for real-time applications, i.e. instantaneous filtering without delay, is hardly possible without digital signal processors (DSPs). With this technology, a powerful DSP can refresh many bandpass filters sequentially in real-time with output (in FAST every 125 ms).

An optimum of filters is reached only as a compromise between slope steepness in the frequency domain and temporal onset and offset. For the specification of fractional band filters, international standards are available [5], in which the frequency curves in the filter pass band and in the attenuation band are fixed with exact tolerances and classifications. Specific requirements are established concerning real-time applications with onset and offset times; and group delays of the different band filters must be considered.

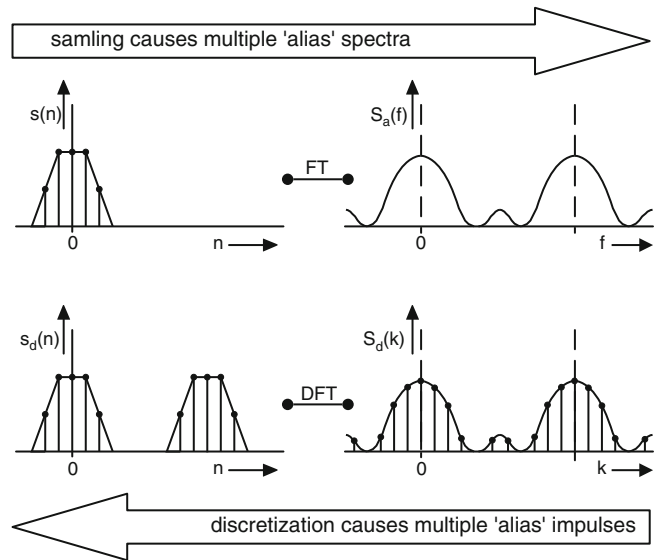
In the case of the quick measurement of spectra that might have a random character, frequency curves in rooms or other systems with high modal density, signals of random noise are advantageous. These allow a direct broadband excitation of the system (e.g., a room, a separating wall, or a muffler) and a direct determination of the band-filtered spectrum. The most general random noise is called 'white noise'. It contains all frequencies with the same amplitude. Also useful is 'pink noise', which contains fewer high frequencies with a slope per octave of  $-3$  dB. It is used if predominantly low frequencies are to be excited and if the tweeter of the measurement loudspeaker should not be overloaded. Due to the energy integrative effect of band filters with increasing frequency (one-third octave, octave), pink noise produces a constant (horizontal) result on the display of a real-time frequency analyser, whereas white noise produces a slope of  $+3$  dB/octave.

The sound pressure level measured has random behaviour due to the random excitation. In order to achieve sufficient accuracy, the averaging time  $T_m$  of the equivalent sound pressure level  $L_{eq}$  must be chosen adequately. The relation between the standard deviation of the level and the measurement duration is estimated by

$$\sigma_L = \frac{4.34}{\sqrt{B \cdot T_m}} \text{dB.} \quad (2.27)$$

where  $B$  = bandwidth of the filter in Hz.

**Fig. 2.13** Discrete Fourier transformation of a time series  $s(n)$  into a line spectrum  $\underline{S}(k)$



## 2.4 FFT-Analysis

### 2.4.1 Sampling of Measurement Signals

In order to obtain signals that can be digitally processed, the voltage signal produced by the microphone must be sampled. This is done by an A/D converter. The fine structure of the process of discretising is dependent on the appropriate time and amplitude resolution. For the hearing range, it is typical to use sampling rates of 44,1 kHz or 48 kHz with a resolution of 16 bits (discretised in steps from  $-32,768$  to  $+32,767$ ). If the sound event to be measured involves a high dynamic range, A/D converters can be found that allow 20 bit or more resolution, so that a 120 dB dynamic range between peak level and quantisation noise can be covered without an amplification switch. The speed of sampling is dependent on the frequency content of the signal. If the sampling frequency is not sufficient to detect fast variations in the signal, sampling artefacts occur that are found in the frequency domain as overlapping 'alias' spectra (aliasing). To avoid aliasing, low pass filters are used that limit the frequency range to, at most, half of the sampling frequency (Nyquist theorem). With regard to the discrete amplitude time function, we have obtained a satisfyingly accurate image of the analogue signal. All further steps such as filtering, analysis, amplification, and storage can now be performed by signal processing much more effectively and with greater variability

(e.g., digital filtering, digital memory devices, Compact Disk, and Digital Audio Tape).

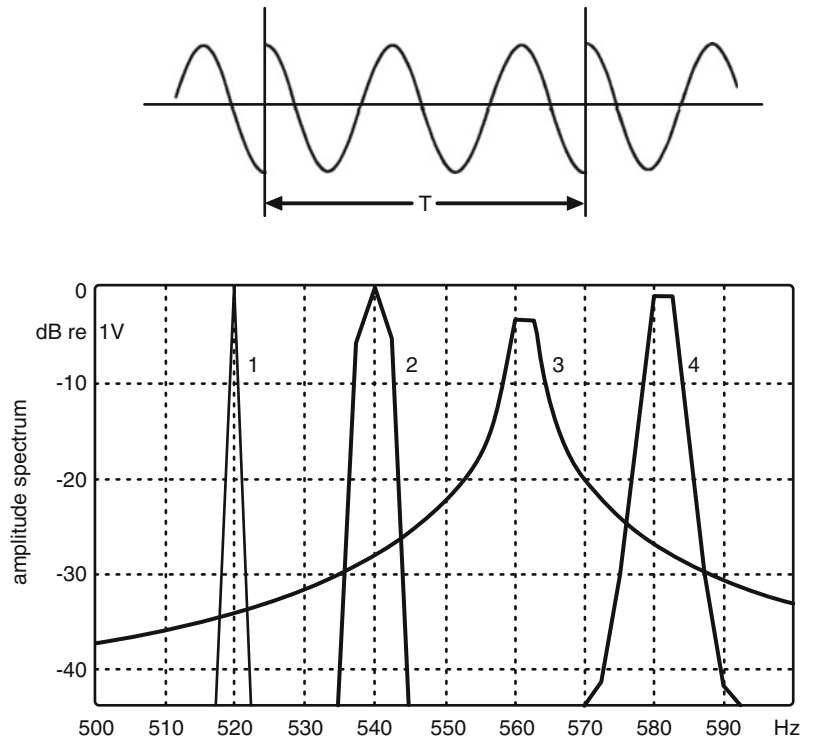
### 2.4.2 Discrete Fourier Transformation (DFT)

Frequency analysis is a very important tool for measurement techniques on acoustic systems. Provided we have sampled time functions, the question is how this data set can be processed efficiently by Fourier transformation. First, we must take into account that the samples are discrete in time, which means that the result of the Fourier transformation will be periodic (see above). The crucial point is that the spectrum to be calculated can only be discrete, too, since a computer memory can only process and store a finite number of spectral lines. Therefore, we must work with line spectra instead of continuous spectra. Line spectra, however, are related to periodic signals only, which gives a second important prerequisite for digital signal analysis: it must be kept in mind that the numerically determined spectra refer to (apparent) periodic time functions (Fig. 2.13).

The discrete Fourier transformation (DFT) can be calculated as follows:

$$\underline{S}(k) = \sum_{n=0}^{N-1} s(n) e^{-j2\pi nk/N}; \quad k = 0, 1, \dots, N-1. \quad (2.28)$$

**Fig. 2.14** (a) Time frame of a pure tone, the period of which is not in an integer number within the time frame; (b) section of the envelope of its line spectrum of harmonics with amplitude 1 V and frequency resolution  $\Delta f = 2.5$  Hz, (1) and (2) signal frequency identical with one of the frequency lines, analysed with (1) rectangular window, (2) Hanning window, (3) and (4) signal frequency in the middle between two frequency lines, analysed with (3) rectangular window and (4) Hanning window



Solving Eq. (2.28) for  $\underline{S}(k)$ ,  $N^2$  (complex) multiplications are required.

### 2.4.3 Fast Fourier Transformation (FFT)

A very powerful variant of the DFT is the Fast Fourier Transformation, FFT. It is not an approximation but a numerically exact solution of Eq. (2.28), which is faster by orders of magnitude. It is, however, only applicable if the number of samples to be transformed is  $N = 2^m$  (4, 8, 16, 32, 64, etc.). The reason for the acceleration compared with the DFT is the reduction of the calculations to the necessary minimum. If we express Eq. (2.28) in terms of a matrix operation, with  $N = 4$ , for example:

$$\begin{pmatrix} S(0) \\ S(1) \\ S(2) \\ S(3) \end{pmatrix} = \begin{pmatrix} W^0 & W^0 & W^0 & W^0 \\ W^0 & W^1 & W^2 & W^3 \\ W^0 & W^2 & W^4 & W^6 \\ W^0 & W^3 & W^6 & W^9 \end{pmatrix} \begin{pmatrix} s(0) \\ s(1) \\ s(2) \\ s(3) \end{pmatrix}. \quad (2.29)$$

we obtain the matrix  $\mathbf{W}$ . It consists of the complex exponential terms of the phasors  $2\pi k/N$  to the power of

$n$ , and it can be rearranged into a form of high symmetry with quadratic blocks ( $2 \times 2$ ,  $4 \times 4$ ,  $8 \times 8$ , etc.) of zeros. The transformation of the matrix means that the vectors must be rearranged, too. The time sequence  $s(n)$  becomes a column vector  $x_1(n)$  (which is called bit reversal, see Eq. (2.30)) and the spectrum vector  $x_2(k)$  is transformed into the final result  $S(k)$ .

The algebraic system to be solved only requires the solution of a sparse matrix equation:

$$\begin{pmatrix} S(0) \\ S(2) \\ S(1) \\ S(3) \end{pmatrix} = \begin{pmatrix} x_2(0) \\ x_2(1) \\ x_2(2) \\ x_2(3) \end{pmatrix} = \begin{pmatrix} 1 & W^0 & 0 & 0 \\ 1 & W^2 & 0 & 0 \\ 0 & 0 & 1 & W^1 \\ 0 & 0 & 1 & W^3 \end{pmatrix} \begin{pmatrix} x_1(0) \\ x_1(1) \\ x_1(2) \\ x_1(3) \end{pmatrix}, \quad (2.30)$$

with  $x_2(0) = x_1(0) + W^0 x_1(1)$ ,  $x_2(1) = x_1(0) + W^2 x_1(1)$  and so on. The latter operations can be illustrated best in terms of a butterfly algorithm, which means that pairs such as  $(x_1(0), x_1(1))$  will

yield pairs  $(x_2(0), x_2(1))$  without the influence of other vector elements. Solving Eq. (2.30) of an  $m \times m$ -matrix can thus be expressed as a cascade of  $m$  butterflies. The total number of operations is reduced from  $N^2$  to  $N \text{ld}(N/2)$ , for example, for  $N = 4,096$  from 16,777,216 to 45,056, which gives a factor of 372. Further possibilities are known for accelerating the algorithm, including strategies of optimal memory access and the fact that real-time signals can be transformed into complex spectra.

#### 2.4.4 Possible Measurement Errors

Under the given conditions for applying FFT, various sources of error are possible. Often, it is forgotten that FFT algorithms, as a special case of the discrete Fourier Transformation, are related to periodic signals only. If a periodic signal (e.g., a pure-tone or triangular signal) is to be analysed, the FFT block length should be equal to an integer number of signal periods. Otherwise, the resulting spectrum will be distorted by the so-called ‘leakage effect’. If the signal ends at a ‘wrong’ sample, the periodic extension will cause a discontinuity. In addition, it is not guaranteed that the fundamental frequency of the signal is represented by exactly one spectrum line (see Fig. 2.15).

If, however, the FFT block length is exactly equal to an integer number of periods, this error will be omitted. Generally, the sampling block of integer number of periods can be mapped to an FFT block length by sampling rate conversion.

An approximate method for error reduction is given by the window technique. A ‘window’ in this sense is a time function with slope onset and offset multiplied

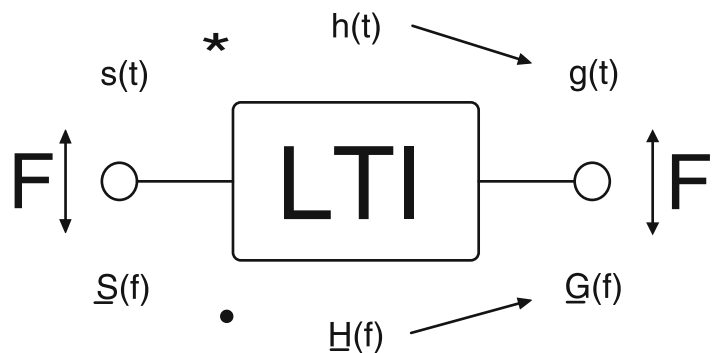
with the signal to be transformed. This corresponds to a convolution of the signal spectrum with the spectrum of the window function. The influence of the discontinuities is thus reduced. The optimal window, however, cannot be specified. The distortions in the spectrum caused by the window can be considered in terms of permissible distortions of spectrum slopes or as permissible side lobes. As a compromise, the so-called ‘Hanning’ window is often used (Fig. 2.14).

$$w(n) = 2 \sin^2 \left( \frac{n}{N} \pi \right). \quad (2.31)$$

#### 2.4.5 Zoom FFT

If a broadband spectrum with a particularly fine structure must be investigated, the Zoom FFT is an appropriate method. Specific parts of the spectrum can be extended in frequency resolution and can thus be evaluated in more detail. This method is based on a shift of the most interesting frequency band,  $f_{\text{low}}$  to  $f_{\text{high}}$ , symmetrically around zero and an analysis of this ‘zoomed’ range with full line density. The frequency shift is gained by the multiplication of a real signal with complex phase vectors  $\exp(-j\pi(f_{\text{low}} + f_{\text{high}})t)$  and low pass filtering. It is worth mentioning that the sampling rate can be reduced significantly because only the number of frequency lines (bandwidth) between  $f_{\text{low}}$  and  $f_{\text{high}}$  must comply with the Nyquist theorem. The general requirement that the line spacing be equal to the temporal block length, however, is still valid. The measurement, therefore, lasts as long as a measurement with the full number of spectral lines.

**Fig. 2.15** Signal path in linear time-invariant systems (LTI). The input signal  $s(t)$  or  $\underline{S}(f)$  and the output signal  $s'(t)$  or  $\underline{S}'(f)$  are related to each other by the response to Dirac pulse (impulse response  $h(t)$ ) or by the response to pure tones (stationary transfer function  $\underline{H}(f)$ ). In the time domain this is realised by convolution (upper path) and in the frequency domain by multiplication (lower path)



### 2.4.6 Advanced Signal Analysis

The analysis using FFT equipment can recover several signal parameters. Accordingly, it makes the detection of correspondence, similarities or separations of signal components possible. Often, it is not ‘just’ a Fourier transformation that is performed, but signal theory provides some interesting methods and results can be gained from FFT and some further operations. One example is the so-called ‘Cepstrum analysis’, which is applied for detecting periodicities in the spectrum, particularly for the analysis of harmonic components in musical acoustics, in machine diagnosis and in speech processing. The Cepstrum is defined as the power spectrum of the (base-10) logarithmic power spectrum:

$$C_s(\tau) = |\mathcal{F}\{\log[|S(f)|^2]\}|^2, \quad (2.32)$$

with

$$S(f) = \mathcal{F}\{s(t)\}; \quad (2.33)$$

the variable,  $\tau$ , called ‘Quefreny’ of the Cepstrum. With  $\mathcal{F}$  we denote formally a Fourier transformation (by FFT, for instance).

Examples of the application of cross-correlation analysis can be found in the calculation of the ‘similarity’ or ‘coherence’ of signals or in the detection of periodicities in signals (auto correlation). The so-called ‘correlation integral’ for a given measurement duration  $T$

$$k_{xy}(\tau) = \int_{-T/2}^{T/2} x(t)y(t+\tau)dt \quad (2.34)$$

can be processed in FFT analysers by the product of Fourier transformations in the form

$$K_{xy}(f) = X^*(f) \cdot Y(f), \quad (2.35)$$

with the frequency functions  $K$ ,  $X$ , and  $Y$  denoting the Fourier transforms of the time functions  $k$ ,  $x$ , and  $y$ ), respectively (between  $-T/2$  and  $T/2$ ).

Generally with (2.37), the overlap is calculated, that is, the parts of the signals which are similar in dependence on the relative time shift  $\tau$ .

$K_{xx}(\tau)$  is called the autocorrelation function.  $K_{xx}(\tau)$  has its maximum at  $\tau = 0$ . If for certain time shifts, values comparable to the maximum (in the normalised definition = 1) appear, the signal is considered periodic (see also Sect. 2.5.4). Stochastic signals are internally uncorrelated and show accordingly very small autocorrelations, apart from  $\tau = 0$ .

From a measurement of two signals over a certain transmission path (for instance, an acoustic transmission line, a vibroacoustic path or an airborne sound path between two points in a room or between two rooms), the complex spectra can be calculated by using an FFT analyser. The characteristics of the transmission path, the complex stationary transfer function  $\underline{H}(f)$  (see Sect. 2.5) can be determined from the cross power spectrum  $K_{xy}(\tau)$ , in spite of the signals being stochastic:

$$\underline{H}(f) = \frac{Y(f)}{\underline{X}(f)} = \frac{Y(f)}{\underline{X}(f)} \cdot \frac{\underline{X}^*(f)}{\underline{X}^*(f)} = \frac{K_{xy}(f)}{K_{xx}(f)} \quad (2.36)$$

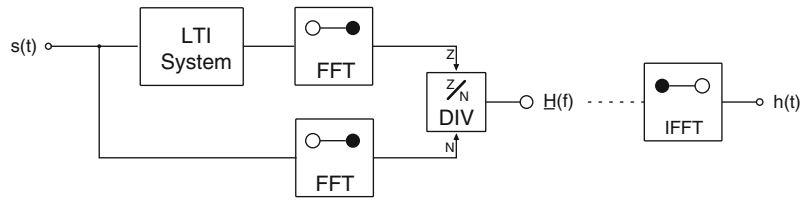
This method of measurement is very effective if one considers stationary random signals from aerodynamic noise sources or any other stochastic process. Measurement tasks in which the excitation signal must be generated are referred to in the description of deterministic periodic signals in Sect. 2.5.

## 2.5 Measurement of Transfer Functions and Impulse Responses

Today, it is no longer a problem to create special test signals using PC-based equipment, to generate and store signals and send them through a DA converter. This offers more flexibility, better power output control and thus higher measurement precision than methods based on stochastic signals and the cross power spectra. The following relationships are very important for performing measurements in which the generation and modification of source signals are explicitly possible.

The device under test shown in Fig. 2.15 is considered a linear time invariant system (LTI). A measurement of the sound transmission through a muffler mounted in a pipe can serve as a basic LTI example. The muffler is located between two microphone positions. Generally speaking, sound transmission is

**Fig. 2.16** Block diagram of the two-channel-FFT-measurement technique



considered from a source position to a receiver position. The electric, acoustic, electro-acoustic or vibroacoustic path between the two points is given by the LTI system.

The assumptions of LTI are the most important prerequisite of the digital measurement technique described here. They are also a prerequisite for the applicability of Fourier analysis (see Sect. 2.4). The consequences of violating these conditions are summarised in Sect. 2.5.5. The condition ‘linearity’ means that the system behaviour is invariant in spite of changes in the input power. Time invariance means that the system does not change over time.

In the figure, too, the logical chain of signal theoretic operations both in the time and frequency domain is illustrated. In each step, these domains are coupled unambiguously through Fourier transformation.

The signal path formulated in the time domain reads (convolution)

$$s'(t) = s(t) * h(t) = \int_{-\infty}^{\infty} s(\tau)h(t - \tau)d\tau. \quad (2.37)$$

The signal path formulated in the frequency domain is

$$\underline{S}'(f) = \underline{S}(f) \cdot \underline{H}(f). \quad (2.38)$$

while the elementary equation for determining system properties in the frequency domain is (see Sect. 2.5.1):

$$\underline{H}(f) = \frac{\underline{S}'(f)}{\underline{S}(f)} = \underline{S}'(f) \cdot \frac{1}{\underline{S}(f)}, \quad (2.39)$$

The same is expressed in the time domain by a so-called ‘de-convolution’

$$h(t) = s'(t) * s^{-1}(t), \quad (2.40)$$

with the signal  $s^{-1}(t)$  being the signal with the inverse spectrum  $1/\underline{S}(f)$ .  $s^{-1}(t)$  is called ‘matched filter’ or transversal filter (see Sect. 2.5.2).

Note: For better understanding, in this chapter the signal transformations and steps of signal processing are expressed in continuous form. In digital instrumentation, the signals are, of course, represented in discrete form [compare Eq. (2.28)].

If  $\underline{S}(f)$  has a white spectrum, we can also write:

$$s^{-1}(t) = s(-t), \quad (2.41)$$

and Eq. (2.34) can be transformed into

$$\begin{aligned} h(t) &= s'(t) * s(-t) = s'(t) \otimes s(t) \\ &\equiv \int_{-\infty}^{\infty} s'(\tau)s(t + \tau)d\tau, \end{aligned} \quad (2.42)$$

which means that  $h(t)$  can also be expressed by cross-correlation of  $s(t)$  and  $s'(t)$  (see Sect. 2.5.3).

Obviously, Eqs. (2.39), (2.40) and (2.42) are equivalent in the case of broadband white excitation signals. Differences exist, however, in the phase spectrum of the excitation signal and the corresponding time sequences. This has a somewhat significant influence on the level adjustment of power amplifiers and loudspeakers. It must be faced that a swept sine and a Dirac pulse have the same magnitude spectra. However, their maximum signal amplitudes are extremely different, although their signal energies are equal.

It is important to note that further consequences of digital representation of signals and spectra must be considered. The finite length,  $T_{\text{rep}}$ , of the deterministic excitation signal and its periodicity is an important factor. The periodicity can well be used for coherent averaging. Periodic signals, however, have a discrete line spectrum with a frequency spacing of

$$\Delta f = \frac{1}{T_{\text{rep}}}. \quad (2.43)$$

Due to the excitation of the system with a periodic signal, the system transfer function is multiplied with a line spectrum. Accordingly, results of the measurement

can only be found at these discrete frequency lines. In addition, the results are not averages over frequency intervals (between the lines, for example), but they are the correct measurement results corresponding to results from pure-tone excitation and high-quality narrow-band filters, for instance. Deterministic periodic signal must, therefore, be strictly separated from stochastic or pseudo-stochastic non-periodic noise signals.

To ensure that the system is in a steady state and that all eventual modes are excited properly, the frequency spacing must be sufficiently dense. One can express the same condition by formulating a requirement for the duration of the signal, which must be long enough to let the system load or decay acoustically. In room acoustics, for example, this is achieved when

$$T_{\text{rep}} \geq T_{\text{rev}}. \quad (2.44)$$

$T_{\text{rev}}$  denotes the reverberation time. Another example is the measurement of resonant systems of the second order with quality,  $Q = 2.2/T$ . Equation (2.47) expresses the fact that the half-width of the mode is covered by at least two frequency lines.

The feature of coherent superposition of signals is used in averaging a number of signal periods. The uncorrelated background noise is added incoherently. Hence, the gain in signal-to-noise ratio by  $N$  averages is

$$\Delta_{\text{av}} = 10 \lg N \text{ dB}. \quad (2.45)$$

More information on the background of digital signal processing for measurements is given in the recent standard ISO 18233 [6].

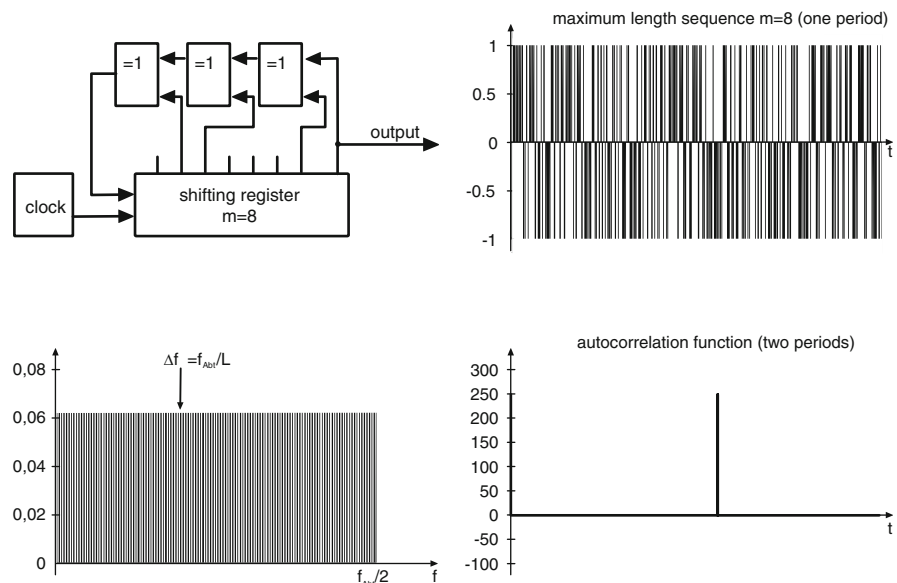
### 2.5.1 2-Channel-FFT Technique

Measurement and the corresponding signal processing are performed in the frequency domain. The same holds for the measurement of transfer functions by using a 2-channel-FFT analyser and the cross power spectrum technique. Input and output signals are measured simultaneously, are FFT transformed and are processed by complex spectrum division Eq. (2.39). An important condition is therefore a sufficiently broad bandwidth, i.e. the excitation signal may not contain 'zeros' in the spectrum to avoid problems in the division. Any periodic signal of length  $2^m$  may be used. For reasons of optimised level adjustment, sweeps, chirps, or deterministic noise do indeed have advantages [7] (Fig. 2.16).

After performing the spectrum division, the impulse response can be calculated from inverse Fourier transformation, if necessary:

$$h(t) = \mathbf{F}^{-1} \{ \underline{H}(\omega) \} = \int_{-\infty}^{\infty} \underline{H}(\omega) e^{j\omega t} d\omega. \quad (2.46)$$

**Fig. 2.17** (a) Generation of a maximum-length sequence with a shift register (example: sequence of order 8 with length 255); (b) one period of the maximum-length sequence; (c) two periods of the autocorrelation function



### 2.5.2 Swept-Sinusoidal Signals

These kinds of excitation signals and the corresponding signal processing are based on the matched filter or transversal filter approach, which includes a direct de-convolution in the time domain Eq. (2.40). The most commonly used signals  $s(t)$  are sweeps, chirps, or time-stretched pulses [8].

The matched filter is determined by inverting the signal sequence in time:

$$s^{-1}(t) = s(T_{\text{Rep}} - t). \quad (2.47)$$

A great advantage of this technique is that the problem of signal periods too short in relation to long impulse responses is avoided. A sequence, short compared with the decay time of the system, is sent only once, while the received signal is recorded over a long duration, which theoretically is infinitely long. This corresponds to an excitation of a (short) signal amended with zeros (zero padding).

### 2.5.3 Correlation Technique

The correlation technique is a special case of impulse measurement techniques. It was originally developed for measuring pulse propagation delays. It can, however, be well used for determining impulse responses and transfer functions. The most important advantage is the possibility of using spread-out signals as measuring impulse responses. The requirements on maximum amplitudes are, thus, significantly relaxed. The domain of impulse responses is not reached directly but only after signal processing.

With direct pulse excitation, the excitation signal approximates a Dirac pulse  $\delta(t)$ . On the receiving side, one measures the impulse response of the system  $h(t)$  directly:

$$s'(t) = \int_{-\infty}^{\infty} h(t')\delta(t-t')dt' \approx h(t). \quad (2.48)$$

In contrast, the convolution integral of the correlation technique reads:

$$\Phi_{ss'}(t) = \int_{-\infty}^{\infty} h(t')\Phi_{ss}(t-t')dt' \approx h(t). \quad (2.49)$$

Rather than the signal  $s(t)$  itself, it contains the autocorrelation function  $\Phi_{ss}(t)$  of the signal and the cross-correlation function  $\Phi_{ss'}(t)$  of the received signal  $s'(t)$  with the excitation. Now, it is not the signal but its autocorrelation function that must approximate a Dirac pulse. This permits much better conditions for level adjustment of the measurement system and the resulting signal-to-noise ratio. However, this advantage must be paid for by having to process the cross-correlation of the received signal  $\Phi_{ss'}(t)$ .

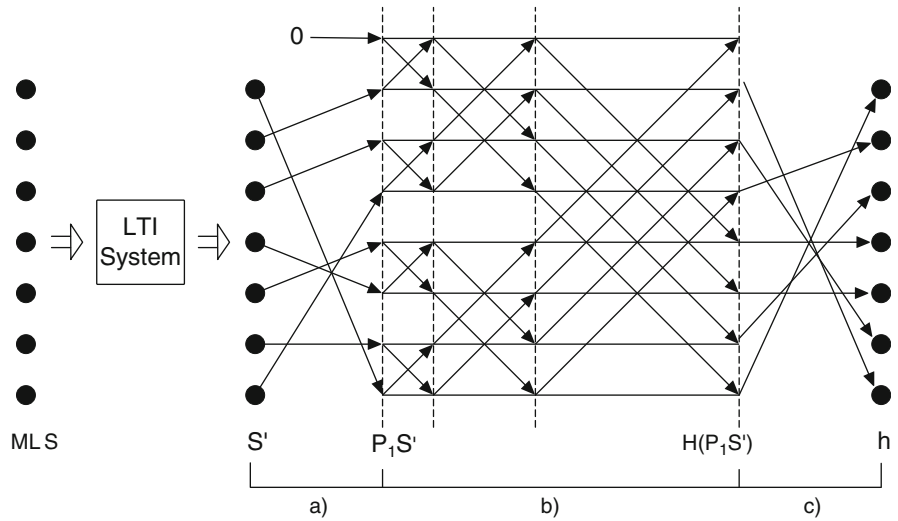
### 2.5.4 Maximum Length Sequences

An important example of correlation signals is maximum length sequences [9]. These are periodic pseudo-random noise signals with an autocorrelation function approximating an almost perfect Dirac pulse. They are generated from a deterministic, exactly reproducible process by using a shift register with feedback. With  $m$  denoting the length (order) of the shift register, a variety of  $L = 2^m - 1$  states is possible. The periodic sequence of maximum length (maximum-length sequence,  $m$ -sequence, MLS) covering all possible states will be achieved under appropriate feedback conditions. For all orders of shift registers, there is at least one feedback rule. In practice, a bipolar excitation signal of '1' corresponds to a positive signal amplitude  $+U_0$  and of '0' to a negative value  $-U_0$ , accordingly (Fig. 2.17).

In commercial frequency analysers, generators of maximum length sequences have been used for quite a long time in order to replace analogue noise generators. The sequence length chosen in these cases is extremely long (typically  $m > 30$ ,  $L > 10^9$ ), so that the periodicity of the signal is no longer recognised. The outstanding property of the signal, i.e. its almost ideal Dirac-like autocorrelation function, is not used to its full capability.

If an LTI system is excited by a stationary MLS signal  $s_{\text{Max}}(t)$ , on the receiving side the convolution  $s_{\text{Max}}(t) \times h(t)$  is recorded. This signal is to be sampled in synchronisation with the clock,  $\Delta t$ , of the shift register. The cross-correlation with the excitation signal Eq. (2.42) is performed by convolution with the time-inverted signal  $s_{\text{Max}}(-t)$ :

**Fig. 2.18** Hadamard transformation of a measured sequence  $s'(n)$ . (a) Permutation of the samples; (b) Hadamard Butterfly; (c) Back permutation in the final time sequence of the impulse response  $h(n)$



$$\begin{aligned} s_{\text{Max}}(t) * h(t) * s_{\text{Max}}(-t) \\ &= s_{\text{Max}}(t) * s_{\text{Max}}(-t) * h(t) \\ &= \Phi_{\text{Max}}(t) * h(t) \approx \delta(t - iL\Delta t) * h(t), \quad (2.50) \end{aligned}$$

with  $i = 0, \pm 1$ , and  $\pm 2$  denoting the sequence counter of periods  $L\Delta t$ .

The autocorrelation function of a stationary periodic maximum-length sequence is a series of pulses of height  $L$  and a small negative offset of  $-1$ . The period is the same as the period of the initial sequence (in the example  $L = 255$ ). Each pulse contains the same energy as the complete maximum-length sequence period. Further enhancement of the signal-to-noise ratio can be achieved by adding  $N$  periods. Due to the strict periodicity of MLS, the amplitudes of the signal must be added, while the background noise is uncorrelated to the signal and adds up quadratically (incoherently). Thus, the signal-to-noise ratio increases according to Eq. (2.45).

In what was stated thus far, the maximum-length sequence offers no specific advantages compared with similar deterministic periodic signals with a smooth amplitude broadband spectrum and low crest factor (ratio of peak value to rms value), such as is described in Sects. 2.5.5.1–2.5.5.2 The interesting point with maximum-length sequences in applications of the impulse measurement technique is a fast cross-correlation algorithm in the time domain. For the calculation of the cross-correlation, we can generally apply either the discrete convolution or the FFT convolution. For a block length  $B$ , the discrete convolution requires  $B^2$ , whereas the FFT convolution requires ‘only’  $B(4 \log_2 B + 1)$  multiplications of complex numbers.

Since the period  $L = 2^m - 1$  of maximum-length sequences is just one sample shorter than the FFT block length, tedious methods for sampling rate conversion must be applied to avoid leakage errors. Much faster is a method for correlation in the time domain, the fast Hadamard transformation (FHT). It is based, like the FFT, on a so-called ‘butterfly’ algorithm and requires no more than  $m 2^m$  additions and subtractions; typically, one obtains an acceleration by a factor 10 compared with FFT-based algorithms.

### 2.5.4.1 Hadamard Transformation

The basis of FHT is the representation of the correlation integral Eq. (2.42) in terms of a matrix operation, i.e. by multiplying a vector with a Hadamard matrix:

$$\bar{\mathbf{h}} = \frac{1}{L+1} \bar{\mathbf{P}}_2 \mathbf{H} (\bar{\mathbf{P}}_1 \bar{\mathbf{s}}'). \quad (2.51)$$

The vector  $s'$  contains the samples of the measured sequence and the vector  $h$  represents the impulse response to be determined. The vectors  $\mathbf{P}_1$  and  $\mathbf{P}_2$  represent permutation rules (see below). A Hadamard matrix  $\mathbf{H}$  is closely related to maximum-length sequences. If we arrange maximum-length sequences in rows one below the other and shifted by one column, we create a matrix that can be transformed into a Hadamard matrix by permutating the columns. Hadamard matrices show interesting features. For instance, they contain a special internal basic structure, which is repeated in several scales (self-similarity). The generation rule for Hadamard matrices of a ‘Sylvester type’ is recursive:

$$\mathbf{H}_1 = 1, \quad \mathbf{H}_{2n} = \begin{pmatrix} \mathbf{H}_n & \mathbf{H}_n \\ \mathbf{H}_n & -\mathbf{H}_n \end{pmatrix}, \quad (2.52)$$

with  $n = 2^m$  and  $m \in \mathbb{N}$ . The crucial point is that products of vectors with Hadamard matrices can be calculated very quickly with a butterfly algorithm, similar to FFT.

Butterfly algorithms process pairs of data in subsequent steps. Thus, the multiplication of the vector with the Hadamard matrix ( $\mathbf{H}\mathbf{P}_1\mathbf{s}'$ ), which normally requires  $2^m(2^m - 1)$  multiplications, can be replaced by  $m \cdot 2^m$  additions and subtractions.

Before this butterfly algorithm can be performed, however, the time sequence to be correlated with the maximum-length sequence must be mapped in an appropriate way to the vector  $\mathbf{s}'$ . This is done by permutation of the samples in the data structure. The permutation rules ( $\mathbf{P}_1$  and  $\mathbf{P}_2$ , see above) are derived from the maximum-length sequence. The complete measurement procedure can be summarised as shown in Fig. 2.18.

An example of applying the correlation technique is the measurement of room impulse responses (reverberation time measurement). The property of impulse compression by the Hadamard transformation and the option to average a number of periods permits measurements at low signal level (for instance, with inaudible signals) and in the presence of an audience during a performance. With increasing averages and increasing signal-to-noise ratios, the time interval useful for the evaluation of room acoustical criteria is becoming larger and larger.

Another advantage of the MLS Hadamard transformation is that it is a very simple method for colouration of the excitation signal. This can be useful for the frequency-dependent optimisation of the level adjustment (for instance, for minimisation of the crest factor) or for implicit equalisation of components of the measurement arrangement. Because of the fact that convolution and cross-correlation are similar except for a time reversal of the signal, a convolution of a maximum-length sequence  $m(t)$  with a filter impulse response  $f(t)$  can be expressed in terms of a correlation:

$$m'(-t) = m(-t) * f(-t) = m(t) \otimes f(-t) = \text{FHT}[f(-t)], \quad (2.53)$$

(convolution) (correlation) (FHT)

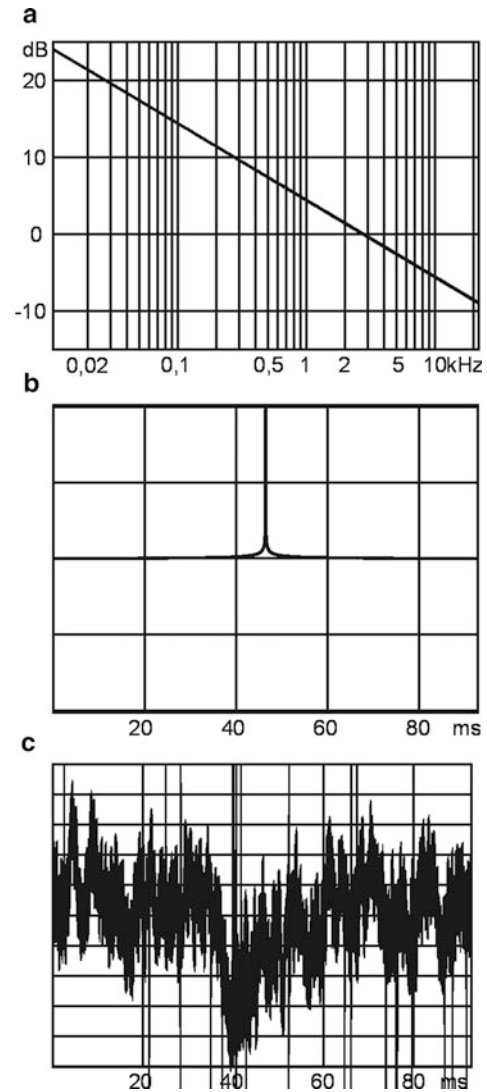
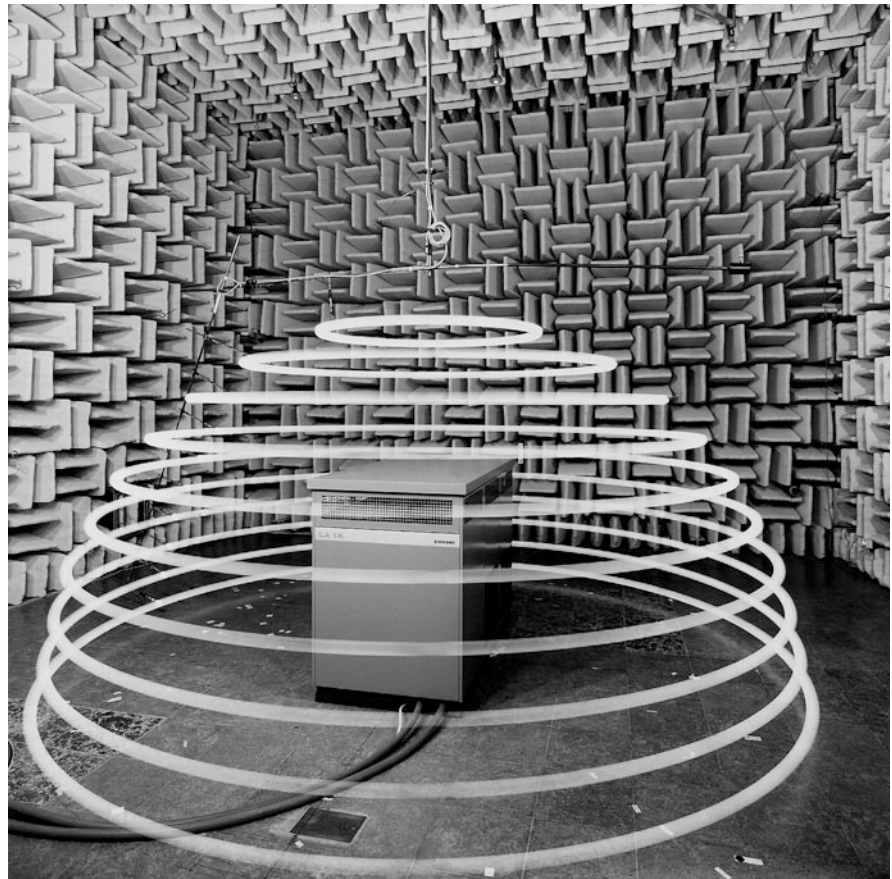


**Fig. 2.19** (a) 'Desired' spectrum of a filter  $F(f)$ ; (b) corresponding impulse response of the filter; (c) corresponding maximum-length sequence with colouration by the chosen filter. Example: 'Pink filter' (linear low-pass function of first order,  $-3$  dB/Octave)

The time-reversed filtered maximum-length sequence  $m'(-t)$  is nothing but the Hadamard transformation of the time-reversed filter impulse response  $f(-t)$ . In order to obtain the filtered maximum-length sequence, the desired filter impulse response must be measured or synthesised, time inverted, then Hadamard-transformed and time inverted again. A Hadamard transformation of this equalised sequence then gives not the ordinary auto-

**Fig. 2.20** Hemi-anechoic chamber (PTB Braunschweig). Example of the surface scanning method for measurement of sound power of a heat pump. The microphone paths of the scanning surface are illustrated by using moving lamps and long-time exposure



correlation function (series of Dirac pulses), but provides directly the previously chosen filter impulse response  $f(t)$  (Fig. 2.19).

### 2.5.5 Sources of Errors in Digital Measurement Techniques

The validity of LTI systems is the most important prerequisite for the usage of cross-spectrum, FFT, or correlation measurement techniques as alternatives for the application of impulsive signals. If non-linearities or time variations cannot be neglected, measurement errors will occur. This holds for the system under test as well as for the measurement instrumentation.

#### 2.5.5.1 Background Noise

Background noise is normally not correlated with the excitation sequence. Thus, impulses as well as pure-tone or broadband stochastic extraneous signals are spread out by the cross-correlation over the complete

measurement duration and are noticeable in the measured impulse response only with their mean power. The parts of the impulse response being dominated by background noise can easily be deleted or filled with ‘zeros’ (window technique, see Sect. 2.4.4). In order to avoid time aliasing, the early part of the impulse response and the necessary decay are to be considered.

#### 2.5.5.2 Non-Linearities

Weak non-linearities can often be tolerated. They appear in the measured impulse response as an apparent noise floor and can hardly be separated from background noise. Accordingly, they are treated like background noise by using the window technique. Non-linearities can be detected by observing the effective signal-to-noise ratio improvement by coherent averaging and by checking if this gain in dynamic range is asymptotically limited. The effect of non-linearities can be reduced by reducing the signal amplitude and the dynamic range can then be further

increased by averaging. Experience has shown that with all methods listed above, signal-to-noise ratios of more than 70 dB can be easily reached. In the case of higher requirements, however, problems must be faced. A further increase of the signal-to-noise ratio is limited by non-linearities in the components of the instrumentation, depending on a clever choice of the excitation signal and on optimal adaptation, on the system to be measured, on power amplifiers, loudspeakers or Sample&Hold devices and A/D converters. Currently, signals with a low crest factor are to be found. Maximum-length sequences are, at first, superior since they have a crest factor of 0 dB. Sweeps and chirps, for example, have a crest factor of 3 dB. Under extreme conditions (signal-to-noise ratio <70 dB), however, maximum-length sequences are not the best choice, due to low-pass components in the digital measurement chain and overshoot effects at the sequence flanks of up to 8 dB. Therefore, their theoretic crest factor cannot be reached in practice. Sweeps or similar signals still keep their theoretical crest factor of 3 dB in electronic realisation and, thus, leave the maximum-length sequences behind.

The FFT and MLS technique are both related to periodic signal processing, whereas the straightforward sweep de-convolution, according to Eqs. (2.40) and (2.47), is related to aperiodic signals. It should be noted that the signal processing related to swept-sinusoidal signals could be performed by the FFT technique as well (see Sect. 2.5.1); thus, periodic or aperiodic algorithms are applicable apparently in free choice. However, the choice of aperiodic signal processing has several practical advantages [7], although related to heavier computational load. Direct aperiodic processing requires de-convolution in the time domain (according to Eq. (2.40) with a sequence of length  $N$ ,  $N^2$  multiplications must be processed). Using a sweep with increasing frequency, the response to harmonic components will appear before the main excitation at that (harmonic) frequency. Accordingly, the harmonic distortion products in the excitation will appear at negative time in the impulse response and may easily be removed by using a time window.

Another important aspect of differences in aperiodic or periodic de-convolution concerns the noise floor in the impulse responses. Periodic processing by FFT or MLS results in an impulse response with a noise floor that is approximately constant, up to the time where the first distortion products appear.

Aperiodic direct de-convolution, however, produces a decaying noise tail that is increasingly low-pass filtered towards its end. This results from the fact that the last part of the impulse response stems from steady-state noise convolved with the excitation sweep in reverse order [see Eq. (2.41)]. One should therefore not interpret the decreasing noise floor as a reverberant tail of the impulse response.

### 2.5.5.3 Time Variances

Time variances do not result in apparent background noise but they do change the signal shape slightly and can, therefore, hardly be detected. Two kinds of time variances are to be discussed: (a) fast variations, which are noticeable within one measurement period, and (b) slow effects, which come into play only in cases of longer averaging. In both cases, a phase distortion in sequences and between sequences is the reason for measurement errors. The coherent averaging and FFT or cross-correlation is affected.

At least some rules or guidelines can be used to avoid the effects of time variances. The result is quite correct if, for instance, it is ensured that maximum temperature drift (degrees Celsius) in a room during the measurement is not larger than

$$\Delta\vartheta < \frac{300}{fT}, \quad (2.54)$$

during a decay measurement with a low level and long averaging time (reverberation time  $T$ , one-third octave band or octave midband frequency  $f$ ). Similar rules of thumb are available concerning the influence of wind.

## 2.6 Measurement Facilities

Connected with various tasks of acoustical measurement and testing, several measurement arrangements, test mock-ups and test rooms are standardised. To obtain acoustic characteristics, acoustic measurements are performed in research regarding biological and medical developments as well as numerous test methods of material testing. The acoustic test arrangements or rooms are implemented to create well-defined acoustic environments.

### 2.6.1 Anechoic Chamber

Spherical waves should propagate as freely as possible, undisturbed by reflections and diffraction (see Sect. 2.1). Measurement rooms fulfilling these conditions are called ‘anechoic chambers’ or ‘free-field rooms’ (Fig. 2.20).

Their walls must absorb sound by 99.9% in order to provide a level reduction of reflections by 30 dB [10]. This requirement is met by mounting wedge-like porous material on the walls and ceiling, either with or without airspace behind. Depending on the dimensions of the wedges, the desired absorption coefficient reached is above 50%. The floor can be treated in the same way (in this case, one enters the room on a net) or the floor stays acoustically ‘hard’ (hemi free-field room).

Besides good free-field conditions, anechoic chambers should have good insulation against background noise. Accordingly, more sophisticated solutions include a vibration-isolated foundation. In this case the room stands on springs, and the low

resonance frequency (depending on room mass and spring stiffness (typically <10 Hz)) hinders vibrations of the surrounding building from outside to propagate into the room.

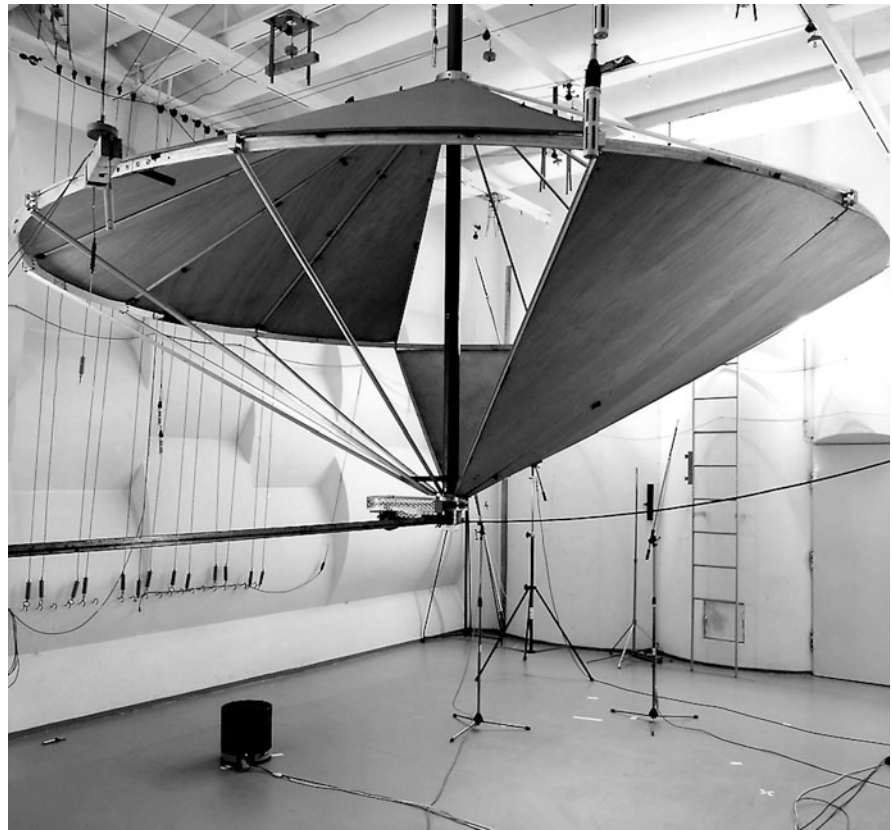
The qualification test of anechoic chambers is performed by the measurement of free field wave propagation, i.e., of the  $1/r$  law, by using various pure-tone signals. Eventually, deviations from the  $1/r$  curve that occur indicate insufficient absorption and, thus, room modes.

Applications for anechoic chambers are all ‘free-field’ measurements on loudspeakers, microphones, hearing aids, noise sources, etc. The frequency response can be determined as well as radiation characteristics and the emitted sound power.

### 2.6.2 Reverberation Room

Diffuse-field conditions can be found in closed rooms, according to the explanations in section XXX ((Room acoustics)). The conditions are, however, not perfectly

**Fig. 2.21** Reverberation room (PTB Braunschweig) with treatment for increased sound diffusivity. (a) Structures on the walls; (b) Rotating diffuser in the room space



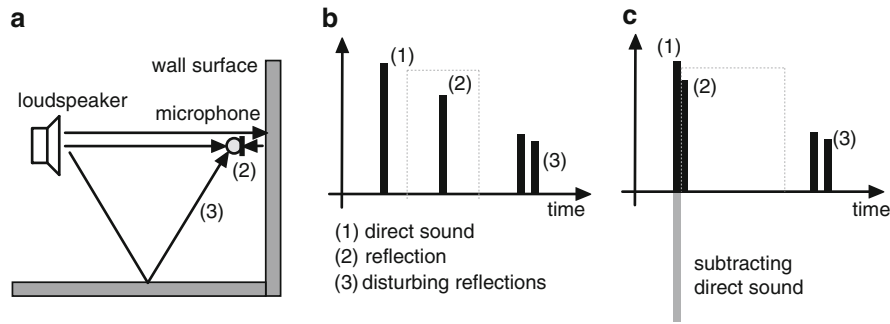


**Fig. 2.22** In situ measurement method for wall impedances and reflection factors. (a) Measurement set-up with reflection paths; (b) Impulse response of this arrangement; (c) Impulse response of the arrangement with the microphone placed close to the surface with time-windowing and direct sound subtraction. The time function of the remaining reflection (2) and Fourier transformation yields the reflection factor  $\underline{R}(f)$

fulfilled due to the statistical superposition of wall reflections or, if the description in the frequency domain is preferred, of room modes.

Prerequisites for diffuse sound fields, however, can be achieved in good approximation if the room boundaries absorb very little energy and if the absorption is uniformly distributed on the walls. The sound field is in this case nearly homogeneous and isotropic. As a further action for ‘mixing’ the sound, non-rectangular rooms and diffusers are used (Fig. 2.21).

The *reverberation room* is in fact the opposite of the anechoic chamber. Its walls should preferably reflect the sound totally. This can be obtained up to a remaining partial absorption of 1–2%, by suitable properties of the air medium and the absorption in a certain layer at the boundaries, even in the case of heavy and smoothly painted walls. At high frequencies, the air absorption is dominant anyway.

For improvement of sound diffusion, the walls of the reverberation room are fitted with sound scattering structures, and some (fixed or rotating) diffusers are placed in the room.

The reverberation times are, therefore, frequency dependent and in a range from above 10 s at low frequencies to about 1 s at high frequencies. Applications for reverberation rooms are measurements of absorption coefficients of materials, of sound power and of diffuse-field sensitivities of transducers.

For the qualification of a reverberation room (quality approval), various theoretical and experimental tests can be performed. At first, the lower frequency limit,  $f_{gr}$ , can be calculated ( $V$  = room volume in  $\text{m}^3$ ,  $T$  = reverberation time in s).

$$f_{gr} \approx 2,000 \sqrt{\frac{T}{V}} \text{ Hz.} \quad (2.55)$$

Below the critical frequency, the conditions of a diffuse sound field are not valid. The modal density is too low and strong spatial variations of energy density are present. One important way to improve the sound field is to add absorption material in order to achieve modal damping and a corresponding larger modal overlap.

In spite of apparently ideal diffuse field conditions, measurements in reverberation rooms must be performed at several source and microphone positions and then averaged, since the sound field is not perfectly homogeneous. Qualification tests of reverberation rooms, therefore, are not based on room geometry but on a selection of source and microphone positions, which yield results with the smallest possible variations around the average value. It must be taken into account that measurements in reverberation rooms are related to broadband incoherent signals analysed in frequency bands and based upon averages  $\langle L \rangle$  of local diffuse-field sound pressure levels  $L_i$  by energetic averaging:

$$\langle L \rangle = 10 \log \frac{1}{N} \sum_{i=1}^N 10^{L_i/10} \text{ dB.} \quad (2.56)$$

Furthermore, in the case of absorption measurements, the sound field in the reverberation room is disturbed by the sample (see section XXX, room acoustics). The requirements of uniform absorption at the room boundaries are no longer fulfilled.

The identification of appropriate positions and averaging procedures is then of particular importance.

## 2.7 Sample Applications

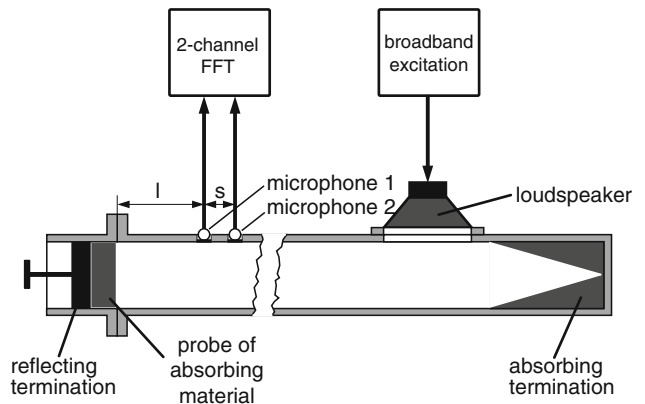
### 2.7.1 Absorption and Impedance

In principle, every method capable of separating incident from reflected waves can be used for measuring the impedances or reflection factors of materials. Accordingly, impulse measurement methods are generally qualified, at least under certain conditions (plane-wave approximation, not-grazing incidence, smooth surfaces and homogeneous impedance distribution on the surface, sufficient time delay between direct sound (1), reflection (2) and disturbing reflections (3), etc.) (Fig. 2.22).

One method requires subtracting the direct sound (part c) which is previously determined under free-field conditions, a time window (broken line) and a Fourier transformation of the remaining reflection component (2), which results directly in the frequency response of the reflection factor.

For obtaining correct results, however, the above-mentioned conditions must be fulfilled. If one or more of these conditions are violated or not even approximately fulfilled, the method should not be applied. Nevertheless, it is the basis for a standardised test method for sound absorption and sound insulation of noise barriers at traffic lines and of road surfaces. In order to account for the simplifications involved in the measurement standard, the results are not denoted as a classical reflection factor,  $R$ , or impedance,  $Z$ , but by the term ‘reflection loss’.

**Fig. 2.23** Impedance tube of the ‘two-microphone method’ for measurement of impedances and reflection factors of material samples and other termination impedances



#### 2.7.1.1 Classical Method (Kundt Tube)

The magnitude of the sound pressure along the tube axis is

$$|p(x)| = \hat{p} \sqrt{1 + |R|^2 + 2|R| \cos(2kx + \gamma)}. \quad (2.57)$$

By investigating the standing wave one can determine

$$|p|_{\max} = \hat{p}(1 + |R|) \quad \text{and} \quad |p|_{\min} = \hat{p}(1 - |R|), \quad (2.58)$$

and thus,  $|R|$ :

$$|R| = \frac{|p|_{\max} - |p|_{\min}}{|p|_{\max} + |p|_{\min}}. \quad (2.59)$$

If  $d_{\min} = |x_{\min}|$  denotes the distance of the first minimum to the wall, the phase

$$\gamma = \pi \left( \frac{d_{\min}}{\lambda/4} - 1 \right), \quad (2.60)$$

can be determined and, according to

$$Z = \rho_0 c \frac{1 + R}{1 - R}, \quad (2.61)$$

the complex sample impedance,  $Z$ . The minima and maxima of the sound pressure of the standing wave are called ‘nodes’ and ‘antinodes’. Positions with maximum sound pressure have minimum sound velocity and vice versa.

In many cases, the intensity loss of reflections is of interest. This is characterised by the absorption coefficient

$$\alpha = \frac{\text{not reflected Intensity}}{\text{incident Intensity}} = 1 - |R|^2. \quad (2.62)$$

### 2.7.1.2 Two-Microphone Method

With the so-called two-microphone method or ‘transfer function method’, impedances and reflection factors can be determined in the broadband approach and much faster (Fig. 2.23). The instrumentation, however, is more complex and the signal evaluation requires a frequency analysis. In this method, it is assumed that the travelling incident wave and the reflected wave can be separated into the spectra  $S_i(f)$ ,  $S_r(f)$  and the reflection factor and that these spectra can be mapped to the transfer function between two points, 1 and 2. For the measured broadband spectra,  $S_1(f)$  and  $S_2(f)$  yield

$$S_1 = e^{jkl} S_i + e^{-jkl} S_r, \quad (2.63)$$

$$S_2 = e^{jkl} e^{jks} S_i + e^{-jkl} e^{-jks} S_r, \quad (2.64)$$

where  $l$  is the distance between the sample and the nearer microphone position and  $s$  is the distance between the microphone positions. By solving these equations, the signal amplitudes and the reflection factor can be calculated:

$$S_i = e^{-jkl} \frac{S_2 - e^{-jks} S_1}{e^{jks} - e^{-jks}}, \quad (2.65)$$

$$S_r = e^{jkl} \frac{e^{jks} S_1 - S_2}{e^{jks} - e^{-jks}}, \quad (2.66)$$

$$R = \frac{S_r}{S_i} = e^{j2kl} \frac{e^{jks} S_1 - S_2}{S_2 - e^{-jks} S_1}. \quad (2.67)$$

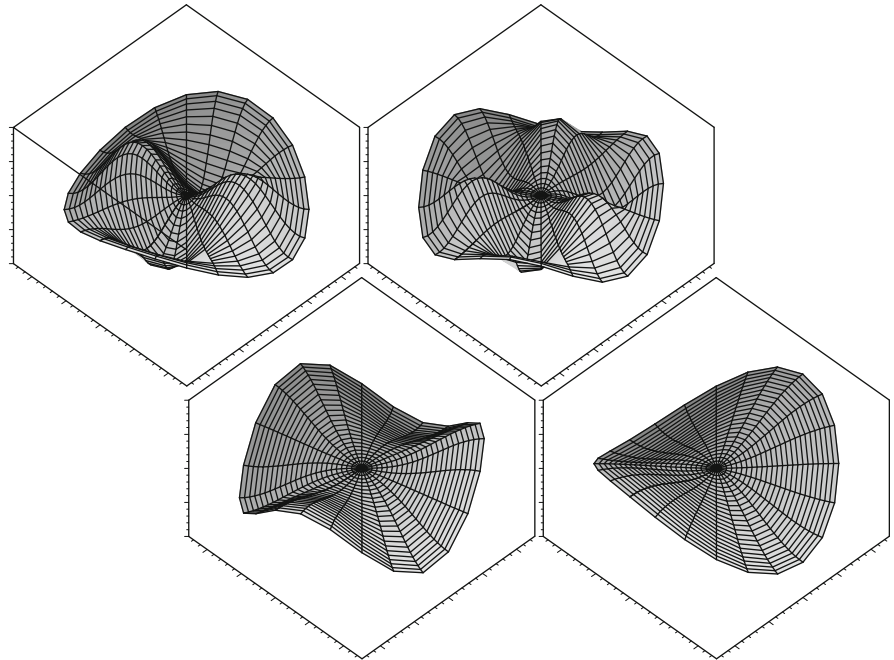
If  $S_1$  is cancelled in the last equation, a representation independent of the absolute spectra  $S_1$  and  $S_2$ ,

$$R = e^{j2kl} \frac{e^{jks} - H_{12}}{H_{12} - e^{-jks}}, \quad (2.68)$$

can be discussed, which contains only the complex transfer function  $H_{12} = S_2/S_1$ .

Requirements on the measurement tube and the instrumentation are specified in detail. The measurement uncertainty is quite small (a few percent), provided the sample is mounted carefully.

**Fig. 2.24** Illustration (animation) of wave forms of a circular membrane. Measurement of vibration velocity and displacement on a grid (mesh) and subsequent processing by modal analysis (four eigenfrequencies)



### 2.7.2 Modal Analysis

Modal analysis is a measurement and evaluation method that provides extended and detailed information. Also here, transfer functions are measured. They are defined between an excitation point and numerous mesh-like located points on structures or in rooms. Such a point mesh must be defined according to the geometry of the object under test, and it must be sufficiently dense according to the highest measurement frequency. As the upper limit of the distance between two mesh points,  $\lambda/6$  is typically used. The transfer functions can be determined on measurements of sound pressure, acceleration or displacement. After the measurement, a computerised evaluation of the measurement data is performed in order to separate the system into specific characteristics in space and time, such as eigenfrequencies (modes) and damping of modes. These modes are mapped to a resonator model based on a set of parameters. Finding the optimal sufficient model and its parameters with best fit to the measured data is the basic task in the method of modal analysis (Fig. 2.24).

Finally, a correlation of the measured peaks with a spatial wave distribution on the mesh opens up the possibility of illustrating each mode at each eigenfrequency in graphical plots and in wave animation. With this method, vibration systems can be analysed and systematically improved.

### 2.7.3 Reciprocal Measurement of Sound Radiation

Measurement of transfer functions [Green's functions  $G(v_n|p_1)$ ] of coupled vibroacoustic problems is essential in noise control. This kind of transfer function is

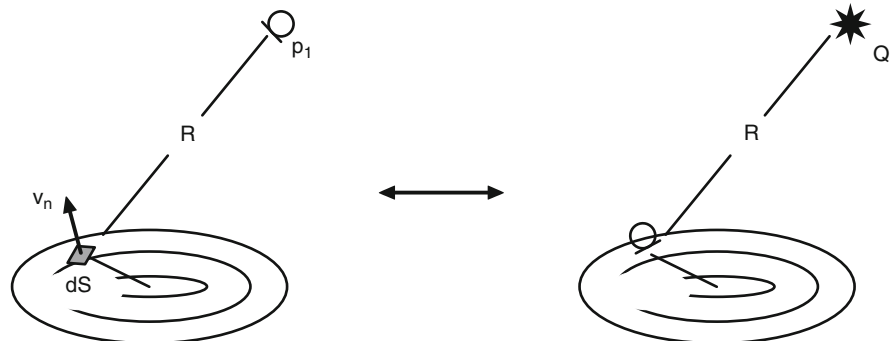
defined as the ratio of the sound pressure measured at a certain field point and the excitation velocity of a vibrating body. However, in practical noise control, the objects of interest are not mathematically simple elements, so that calculation methods cannot be used at all, except numerical methods such as FEM, BEM, etc. For discussion of some more details of the theoretical foundations, it should be emphasised that two measurement methods can yield the same results if the reciprocity between sound radiation and sound reception is exploited [11] (see also Sect. 2.2.4.2) (Fig. 2.25).

$$\frac{p_1}{v_n dS} = j\omega\rho_0 G(v_n|p_1) = \frac{p_2}{Q}. \quad (2.69)$$

A surface element  $dS$  of a radiating body is considered as point source on an otherwise rigid body. The transfer function between the normal component of the velocity on  $dS$  and the sound pressure at the field point is identical with the transfer function between the volume flow of a (volume) source placed at the field point and the sound pressure near the rigidly fixed surface element. Provided the problem was solved for a specific surface element, the complete solution consists in a superposition of all surface contributions. Needless to say, the transfer functions are complex and all modern digital measurement methods with FFT, sweeps or correlation techniques can be applied.

The fact that the measurement can be performed in two directions opens enormous advantages, particularly if sound velocities of vibration surface elements cannot be detected with optical sensors or accelerometers but rather easily by piezoceramic pressure sensors, for instance, in measurements of sound radiation from components or machines under extreme conditions of temperature, moisture, or with highly

**Fig. 2.25** Reciprocity principle: Equivalence of sound radiation (left) and sound reception (right). The transfer function for the distance  $R$  is called Green's function; it can be interpreted as acoustic transfer impedance



reactive gases. Another example is the sound radiation of tyres. Measurement by scanning the sound pressure near the tyre is much easier than measuring the normal velocity of the tyre surface.

---

## References

1. De Bree H-E (2003) An overview of microflow technologies. *Acta Acustica United Acustica* 89:163
2. Bjor O-H (1982) Schnellemikrofon für Intensitätsmessungen. FASE/DAGA 82 – Fortschritte der Akustik, Göttingen, 629
3. Kuttruff H, Schmitz A (1994) Measurement of sound intensity by means of multi-microphone probes. *Acustica* 80:388
4. IEC 61043 (1993) Electroacoustics – Instruments for the measurement of sound intensity – Measurements with pairs of pressure sensing microphones
5. IEC 61260 (1995) Electroacoustics – Octave-band and fractional-octave-band filters
6. ISO 18233 (to be published) Acoustics – Application of new measurement methods in building acoustics
7. Müller S, Massarani P (2001) Transfer-function measurement with sweeps. *J Audio Eng Soc* 49:443
8. Aoshima N (1980) Computer-generated pulse signal applied for sound measurement. *J Acoust Soc Am* 69:179
9. Rife D, Vanderkooy J (1989) Transfer-function measurement with maximum-length sequences. *J Audio Eng Soc* 37:419
10. Mechel FP (1998) Schallabsorber, Band III. S. Hirzel Verlag, Stuttgart, Kap. 4
11. Fahy FJ (1995) The vibro-acoustic reciprocity principle and applications to noise control. *Acustica* 81:544



<http://www.springer.com/978-3-540-24052-5>

Handbook of Engineering Acoustics

Müller, G.; Möser, M. (Eds.)

2013, X, 702 p. 457 illus., Hardcover

ISBN: 978-3-540-24052-5